CLSS: 00056

a0010

Milankovitch theory in the Earth System

Mathis P Hain[a,b] and Daniel M Sigman[c], [a]University of California, Earth and Planetary Sciences, Santa Cruz, CA, United States; [b]University of California, Ocean Science, Santa Cruz, CA, United States; [c]Princeton University, Department of Geosciences, Princeton, NJ, United States

Abstract

In the early 20th century, Milutin Milankovitch revisited and formalized the hypothesis that "ice age" episodes of alpine glacier advance were caused by slow but regular changes in Earth's orbit around the Sun. In the mid-1900s, climate reconstructions provided the first empirical support for a link between orbit and climate, with Milankovitch's specific orbital hypothesis offering promise to explain Northern Hemisphere glacial changes. However, ice ages were found to exhibit global rather than regional cooling—in contrast to "Milankovitch theory"—indicating that other processes must also be involved. In the 1980s, reconstructions of recurring ice age changes in ocean circulation and atmospheric carbon dioxide (CO_2) promised to provide the missing ingredients, with the latter specifically involving the CO_2-driven greenhouse effect. This chapter focuses on how new reconstructions, models and statistical tests have changed our understanding both of Milankovitch theory and of the carbon cycle dynamics that acted to amplify and globalize glacial/interglacial climate cycles.

Key points

u0010 - We outline the historical context of classical Milankovitch theory and the mechanisms it contains to link Earth's orbit to the rhythm of recurring ice ages.
u0015 - We survey dynamic changes in ice sheets, ocean circulation, carbon cycle and climate variability that moderate the climate response to orbital forcing.
u0020 - We highlight outstanding questions regarding the total Earth System response to geologic, orbital and stochastic climate forcings.

s0015 ## Introduction

p0030 Humans have seemingly always looked to the sky in search of divine influence on events in their natural environment, assigning specific meaning to the Sun, the moon, the wandering stars and the fixed stars. These notions culminated in the Copernican revolution placing the Sun in the center of our solar system, with Earth and the wandering stars each following their own elliptical orbit with the Sun in the focus point. In the 18th and 19th century, when the new field of Geology developed striking evidence for past climate change across eons of deep time, scientists sought mechanistic and deterministic explanations for these drastic environmental changes. It was found that Earth most recently experienced "ice age" advances of alpine mountain glaciers and northern ice sheets that deposited gravels, boulders and shaped moraines into the modern landscapes (Esmark, 1824; Venetz, 1833; Schimper, 1837; Agassiz, 1840; Torell, 1872, 1873, 1875; Geike, 1894; cf. Fleming, 1998; Krüger, 2013) and that distinct phases of ice age glaciation were separated by intervening "interglacial" warm periods (Penck, 1879; Chamberlin, 1894). Evolving alongside this geologic evidence, early theories considered how Earth's orbit around and its orientation toward the Sun might have differed in the past to cause the last ice age (Esmark, 1824; Herschel, 1832), and later how cyclical changes in Earth's orbit and orientation may have caused repeated glacial-interglacial cycles (Adhémar, 1842; Croll, 1864, 1875; Pilgrim, 1904). It is this line of research that Milutin Milankovitch (1879–1958) championed, making "Milankovitch theory" synonymous with the orbital theories aimed at explaining ice ages.

p0035 Milankovitch developed a mathematical framework to compute how the influence of the other solar system bodies effected changes in daily, seasonal and annual solar insolation received by Earth at different geographic latitudes. Further, Milankovitch advanced a climatology based on the daily and seasonal balance between absorbed insolation and outgoing thermal radiation, whereby low summer-season insolation at 65° northern latitude causes cool summers and persistence of reflective snow cover in high northern latitude, which in turn causes regional cooling, snowline lowering and the initiation of continental ice sheets in the high latitude northern hemisphere. Finally, Milankovitch estimated that, by reflecting sunlight to space, the ice sheets themselves would have an indirect cooling effect that is highly concentrated in the region immediately adjacent to the northern ice sheets, sufficient to explain landform evidence for the repeated down-valley advance of mountain glaciers[1] in the European Alps (44–48°N). On this basis, Milankovitch induced that low 65°N summer insulation was "enough to cause ice ages"[2] and that:

> "[. . .] the presented solution to the ice age problem yields a new problem, that is, why did orbital insolation forcing not cause similar glaciations before the last 800 thousand years." – Milankovitch, (1930, p.A175). dq0010

p0040 While it was later found that recent ice ages were indisputably influenced by orbital insolation forcing (Hays et al., 1976; Imbrie et al., 1984), the narrow view of ice ages as regional phenomena that were immediately and exclusively caused by insolation changes was questionable from the beginning (Penck, 1938; Milankovitch, 1941), and it is no longer tenable in light of modern observations and models (Imbrie et al., 1993; Paillard, 1998). For example, recent ice ages became progressively more severe across multiple cycles of low northern summer-season insolation (Broecker and Van Donk, 1970). Moreover, when ice volume finally reached a maximum at the peak of the last ice age, cooling was global rather than regional ("ice age as times of general cooling, including the tropics"; cf. Penck, 1938, p.349; CLIMAP, 1976; Tierney et al., 2020). Neither of these observations is explained by Milankovitch's mechanism for ice ages. In addition, it was discovered that warming at the end of the last ice age initiated in the Southern Hemisphere (Bender et al., 1994; Sowers and Bender, 1995; Blunier et al., 1998; Blunier and Brook, 2001; Shakun et al., 2012), thousands of years (millennia, in units of *kyr* for duration and *ka* for absolute age) before abrupt warming and ice sheet disintegration in northern high-latitudes (Deschamps et al., 2012; Snoll et al., 2024; Hines et al., 2025). There is also evidence that ice age climate cycles evolved independently from orbital forcing (Paillard, 2001; Lisiecki and Raymo, 2005; Chalk et al., 2017). Thus, it remains an outstanding challenge to mechanistically connect orbit-driven changes in insolation with Earth's reconstructed climate history.

p0045 After a brief review of the historical context of orbital theories for ice ages, we turn to the dynamical elements of the Earth System that were theorized at the time but not fully considered by Milankovitch: (1) the glaciologic dynamics affecting ice sheet response to forcing, (2) the response of surface temperature, winds and ocean circulation to forcing, (3) the carbon cycle feedbacks that regulate atmospheric CO_2 climate forcing in response to changes in ice sheets, climate and ocean circulation. In addition, (4) we consider the continuum climate variability that emerges from slow-acting feedbacks in the Earth System. We summarize the perspective that ice age cycles are not simply the product of orbital forcing of ice sheets, as the ice age cooling cannot be explained without the coupled action of ocean circulation and the global carbon cycle. Moreover, we observe an important role for chaotic millennial-scale variability in ocean circulation and atmospheric CO_2 in the chain of events that ended recent ice ages. Lastly, secular trends in ocean circulation, carbon cycle, the progressive development of the ice sheets, and their transformation of Earth's landscapes are implicated in the evolution of the ice age cycles through time.

s0020 Earth orbit, insolation and climate

s0025 Earth orbit

p0050 Structures built in antiquity frequently appear to be aligned with the stars, such as Stonehenge, which defines a visual axis that connects sunrise on the longest day of the year (summer solstice) with sunset on the shortest day (winter solstice). Indeed, humans have stargazed since at least the Stone Age, for such diverse purposes as time-telling, navigation and spirituality. When an entirely new (fixed) star became visible over the southern horizon of the Mesopotamian city of Eridu some 6000 years ago, word spread quickly, but it would take another 200 years for it to become visible in the more northern city of Uruk (Bautsch and Pedde, 2023). Ancient cultures also tracked the movements of "wandering stars" (ancient Greek πλανῆται; latin *planetae*; i.e., the planets). Moreover, observers in several cultures noticed that the position of the fixed stars as seen during equinox appeared to shift gradually over time, with ancient Greeks developing a cosmology with the celestial objects affixed to "orbs" that rotate about Earth, which was perceived as the unmoving center of the universe. This geocentric system was able to predict the ascent of the wandering stars, with some inaccuracies, contradictions, and complications. Recognizing these shortcomings, 16th century scholar Nicolaus Copernicus formulated a new cosmology that had the Sun at its center, with Earth and the other planets moving on concentric orbits around the Sun. This new view of the world was confirmed and refined when Johannes Kepler found the planets to follow elliptical orbits,

[1] Milankovitch (1930), p.A170: "Due to this [insolation-induced] reduction of summer temperature, the snowline was shifted by a mean of 700 to 800m lower than at present. Wide-ranging areas thereby became covered by an ice blanket lasting through summer and glaciers advanced to conquer the valleys."

[2] Milankovitch (1941; p.616f) "[According to Penck, 1938 . . .] secular insolation changes are incapable to quantitatively explain the large climates swings of the Quaternary. The calculations reported here contradict that perspective. When accounting for the changing reflectivity of Earth, insolation changes are enough, as proven by the numbers, to completely explain even the larges climatic events of the Quaternary and to clarify their cause [Ursache]."

moving faster when closest to the Sun (perihelion) and slowest when furthest away (aphelion). The Copernican revolution in understanding Earth's place in our solar system was completed when Isaac Newton generalized Kepler's laws of planetary motion to infer the law of gravitation, defining the force that keeps the planets on their elliptical orbits around the Sun.

p0055 With the general notion of planetary motion settled, Newton shifted attention to the problem of the stability of planetary orbits and the solar system, leading to advances in mathematics that allowed calculation of the gravitational attractions among the planets (e.g., Le Verrier, 1846) that act to change their orbits over time to make them more or less elliptical (increasing and decreasing their orbital eccentricity). For Earth, this results in a short (100-kyr) and a long (400-kyr) eccentricity cycle (Fig. 1A left). The attraction of the planets on each other causes their elliptical orbits to gradually rotate around the Sun ("apsidal precession," Fig. 1A center). In addition, it was found that Earth's rotation flattens the shape of Earth (and the other planets) at the poles to create an equatorial bulge that is tilted with respect to Earth's orbit and hence creates a torque when subject to gravitation (as from moons), so that Earth's inclined spin axis gradually describes a circle around the normal of Earth's orbit (axial precession of the Earth-Moon system; Fig. 1B left; Wu et al., 2024). It is this "axial precession" that primarily causes the gradual shift of fixed stars at equinox observed since antiquity. Earth's axial precession is toward the apsidal precession of Earth's orbit, yielding a ~ 21-ky precession of the equinox (Fig. 1C left), Moreover, the orbits of Venus, Earth, Jupiter and Saturn are all slightly tilted relative to the Laplace plane of the solar system (i.e., the plane defined by the angular momentum vector of our solar system as a whole), with the normal to their orbits precessing around the normal of the Laplace plane (precession of the ascending node) as required by conservation of the angular momentum of the solar system. Finally, because Earth's and Venus's spin axis movements are tightly coupled by conservation of angular momentum (Rainey, 2021), both axes describe coordinated precession motions relative to the Laplace plane (Fig. 1B right), resulting in dominant periods of 72-kyr and 50-kyr, the latter arising from interference by Jupiter and Saturn (cf. Fig. 4 and equation 30 in Rainey, 2022). The precession of the Earth-Jupiter system (Fig. 1B right) is slower than and away from the axial precession movement (Fig. 1B left). Taken together, the interactions act to change the tilt of Earth's spin-axis relative to the normal of Earth's orbit with a dominant 41-kyr and lesser 54-kyr periodicity (Fig. 1C right)—commonly referred to as Earth's obliquity.

s0030 Orbit, insolation, and climate

p0060 We experience Earth's orbit relative to the Sun, with the daily cycle of Earth's rotation and the seasonal cycle of each year that Earth orbits the Sun. For that reason, orbital forcing of climate manifests as gradual changes in the intensity of daily solar insolation and the duration of the different seasons (Chiang and Broccoli, 2024). Taking the 2025 orbit as an example, it takes 88.9 days from winter solstice to spring equinox (Dec. 21st to March 20th), 92.7 additional days to summer solstice (June 20th), 93.7 additional days to Autumn equinox (Sep. 22nd), and 89.9 additional days back to winter solstice; for a total of about 365.25 calendar days per astronomical year (hence the leap years proposed by Julius Cesar in 46 BCE). Moreover, in 2025, Earth's closest and furthest distance from the Sun fell on Jan. 4th (147 million km) and July 3rd (152 million km). In the Northern Hemisphere, the seasonal distance and orbital speed changes yield slightly stronger winter daily insolation but shorten the winter season while slightly strengthening summer daily insolation but lengthening the summer (and the reverse in the Southern Hemisphere; Fig. 1C left). Over time, these dates gradually shift relative to each other and relative to our calendar, thereby changing how sunlight is distributed over the year.

p0065 The Northern Hemisphere has more spring/summer than autumn/winter days and hence more annual hours of daylight than nighttime, and the reverse applies to the Southern Hemisphere. On that basis, Adhémar (1842) proposed that the current orbit produces long Southern Hemisphere winters and hence favors glaciation of Antarctica, but that precession of the equinox would periodically reverse the hemispheric bias in daylight hours so as to cause northern glaciation, i.e., the recurring ice ages discussed at the time (Schimper, 1837; Agassiz, 1840). This idea of orbitally forced climate had a mixed reception (Krüger, 2013), in part because Alexander von Humboldt pointed out (cf., Krüger, 2013, p.482) that seasons are longer when Earth is farthest from the Sun (aphelion), with relatively weaker intensity of daylight (i.e., stronger insolation during short seasons), such that both hemispheres receive almost equal annual average insolation. Croll (1864) further advanced Adhémar's orbital theory of ice ages by recognizing that a long winter with weak insolation would be a cold winter and that the change in insolation seasonality due to precession is stronger when Earth's orbit is more eccentric (with a greater difference in distance to Sun between aphelion and perihelion, Fig. 1A left; (Croll, 1867)). He also proposed that the climate response to this orbital forcing could be amplified by positive feedback mechanisms,[3] pointing to the high reflectivity (albedo) of snow and ice and speculating about ocean circulation changes (Thompson, 2021). Specifically, Croll realized that a modest cooling caused by orbital insolation forcing can lead to increased snow and ice cover of the landscape, the high albedo of which leads to less solar radiation absorption and, thus, further cooling—the concept of a strongly positive (amplifying) ice–albedo feedback regulating regional temperature change. Changes in Earth's obliquity (Fig. 1C right) did not feature in Adhémar's orbital theory, were only outlined in Croll's work, and were not included in the synthesis orbital solutions by Le Verrier (1846) and Stockwell (1873). It was Pilgrim (1904) who first set out to

[3]Croll (1875), p.52: *"There is one remarkable circumstance connected with those physical causes [of ice ages] which deserves special notice. They not only all lead to one result, viz., an accumulation of snow and ice, but they react on one another. It is quite a common thing in physics for the effect to react on the cause. In electricity and magnetism, for example, cause and effect in almost every case mutually act and react upon each other. But it is usually, if not universally, the case that the reaction of the effect tends to weaken the cause. The weakening influences of this reaction tend to impose a limit on the efficiency of the cause. But, strange to say, in regard to the physical causes concerned in the bringing about of the glacial condition of climate, cause and effect mutually reacted so as to strengthen each other. And this circumstance had a great deal to do with the extraordinary results produced."*

CLSS: 00056

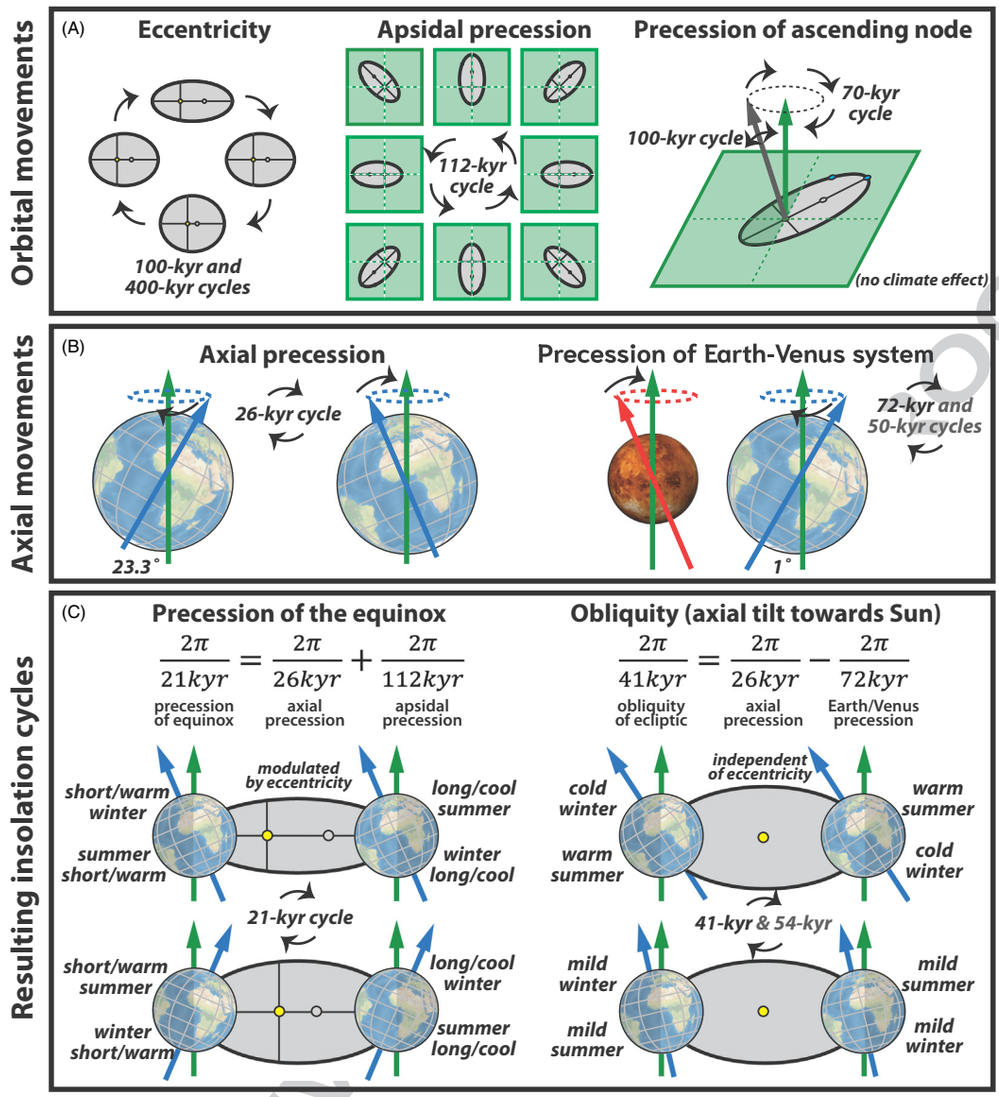

f0010 **Fig. 1** Illustration of (A) cyclical movements in Earth's annual orbit, (B) of Earth's rotation axis orientation, and (C) the resulting seasonal insolation changes that affect Earth's climate, highlighting the causal relationship between Earth's orbit and seasonal climates. (A, left) The gravitational attraction among planets causes Earth's orbit to deviate from being circular on a cyclic basis. The "eccentricity" of its elliptical orbit refers to the distance between the two focus points of the orbit, one of which is occupied by the Sun (yellow dot). There are eccentricity cycles of both 100 kyr and 400 kyr period. (A, center) Aphelion and perihelion (farthest and closest points to Sun) take a 112-kyr period of apsidal precession to rotate relative to the fixed stars (our galaxy) on the plane of the solar system (i.e., the Laplace plane, shown as a green square with its normal vector as green arrow). (A, right) The slight tilt of the normal of Earth's orbit (black arrow) relative to the normal of the Laplace plane (green arrow) oscillates with a 100-kyr period, and the direction of tilt rotates with a 70-kyr period relative to the fixed stars. (B) Earth's rotation on its axis (blue arrow) causes an equatorial bulge that attracts a torque by gravitation with Moon and Sun. (B, left) The movement of the Earth-Moon system and of Earth's rotation axis describes a 26-kyr circle (axial precession) around the Laplace normal (green arrow) relative to the fixed stars, as noted by observers in antiquity. In addition, (B, right) the tilts of the rotation axes relative to the Laplace plane of Venus and the Earth-Moon system are tightly coupled by conservation of angular momentum, with a dominant period of 72 kyr and a secondary period of 50 kyr that is excited by torque from Jupiter and Saturn (Rainey, 2021, 2022). Earth's spin axis is hence tilted in two directions: ~23.3° with respect to the Moon's orbit and ~1° with respect to corresponding tilt of Venus. These factors combine to lead to two dominant orbital cycles in the annual cycle of insolation of solar radiation received by Earth (C). First, (C, left) apsidal and axial precession (panels A and B, respectively) are toward each other, shortening the climatologically meaningful *precession of the equinox* so that its period is an average of only 21 kyr. Second, (C, right) the tilt axial precession and the precession of the Earth-Venus system are both clockwise, yielding a dominant 41-kyr and a weaker 54-kyr cycle for Earth's *obliquity of the ecliptic* (i.e., the net tilt of Earth's axis relative to Laplace normal and Sun). Precession of the equinox shifts local insolation between seasons, an effect that is stronger when orbital eccentricity is greater and insignificant when the orbit is nearly circular, every 100 kyr. Low obliquity yields mild seasons at any given latitude while producing a larger annual average insolation contrast between the tropics and the polar regions, independent of the orbit's eccentricity, with minimal insolation effects on mid-latitude regions such as the European Alps. In common usage, "climatic precession" (of the equinox) and "obliquity" (of the ecliptic) are described as separate phenomena with distinct climatic effects. Milankovitch theory does not explicitly distinguish between precession and obliquity but instead focuses on their combined effect on summer-season insolation received at "boreal" high northern latitudes (i.e., 65°N), which is significantly affected by all orbital parameters (A and B) except precession of the ascending node (A, right).

compute and tabulate, for the last million years, all three orbital elements that determine Earth's insolation (Fig. 1B). With this initial input, Milankovitch calculated the corresponding changes in seasonal insolation at various latitudes and then explored their implications for temperature and land ice in an effort to explain the evidence of past Northern Hemisphere glacial advances (Berger, 2021, Fig. 1C).

p0070 Milankovitch's successively refined insolation curves (Milankovitch, 1920, 1930, 1941) demonstrated the precession-driven changes that yield long and cold winters alternating in a 21-kyr cycle between the hemispheres (cf. Adhémar, 1842; Croll, 1864) as well as a distinct 41-kyr cycle of annual insolation being either concentrated in the tropics during low obliquity, or being extended into the polar regions of both hemispheres during high obliquity (i.e., a combination of Fig. 1C left and right). That is, precession of the equinox redistributes insolation between the seasons without changing the annual average, while obliquity redistributes annual average insolation between the tropics and the polar regions; neither cycle significantly changes the global annual average. Milankovitch recognized that the effect of low obliquity would primarily be summertime cooling in the polar regions. With the encouragement of Wladimir Köppen, he broke with the Adhémar/Croll theory that cold/long winters favor ice ages and instead hypothesized that low summertime insolation in the boreal zone (i.e., ~65°N) would have facilitated the recurring initiation and growth of continental ice sheets in Scandinavia and North America (Brückner et al., 1925). Known terminal moraines from past down-valley advance of Alpine glaciers offered a temperature reconstruction by comparison to modern glaciers and could be dated by cross-cutting relationships and relative stages of colonization of glacial boulders by lichen, at the time offering the best available geologic test for the orbital theories of ice ages. Milankovitch recognized that the influence of obliquity on summer insolation was weak at the latitude of the Alps and that the local summer insolation changes were too weak to explain the ~5 °C cooling suggested by the moraines. Based on these considerations and in consultation with his colleagues Köppen and Wegener, Milankovitch (1930) advanced the mechanistic theory that low boreal summer insolation (at 65°N) allows snow cover to persist through the summer to accumulate year-on-year and so form northern ice sheets. In his later work, Milankovitch (1941) used global snowline data compiled by Köppen (in Wegener, 1929) to further rationalize a boreal summer insolation threshold for ice sheet initiations, where snow and ice reflecting more sunlight back to space would more than double the local summer insolation forcing that results from orbital change alone; effectively including Croll's ice–albedo feedback but specifically tied to boreal summer-season insolation. This indirect albedo cooling effect would only impact the immediate vicinity of the northern ice sheets and thereby cause regional ice ages.[4] As such, Milankovitch explained the timing of Alpine glaciers' down-valley advances when low obliquity favors boreal ice sheets that cause regional cooling (obliquity having minimal direct effect on insolation at the latitude of the Alps), aphelion coincides with summer solstice (yielding cool although long northern summers), and orbit eccentricity is high.

p0075 In modern reconstructions of the ice age climate cycles (Fig. 2) obliquity-period (41 kyr) variability is substantially stronger than variability with precession period (21 kyr) (Hays et al., 1976; Ruddiman et al., 1986; Lisiecki and Raymo, 2005), validating the core tenant of Milankovitch theory. Modern dating of Alpine moraines is in remarkable agreement with Milankovitch's age assignments, and climate models support Milankovitch's argument that the regional cooling of the Alps was dominated by the ice-albedo cooling effect of boreal ice sheets (Zhu and Poulsen, 2021). But with the benefit of modern observations and models, the research community has found that Milankovitch's core proposals fail to address important aspects of the ice age cycles (Paillard, 2001; Berger, 2013, 2021). One problem is that the significant precession component of boreal summer insolation (at 65°N) is proportionally minor in the climate record (Fig. 2B). Explanations for its particular absence before ~1 Ma include (1) an explicit temperature threshold for summer-season melting (Huybers and Tziperman, 2008) broadly similar to Milankovitch mechanistic theory, and (2) cancelation of precession-driven ice sheet melting between the hemispheres (Raymo et al., 2006) more similar to Adhémar's theory. After ~1 Ma, precession remains a proportionally minor periodicity (Fig. 2B), but there are signs of precession's importance in the specific timings of the major deglaciations (Kawamura et al., 2007; Suwa and Bender, 2008) and in other aspects as well. A second problem is that the intensification of Northern Hemisphere Glaciation (iNHG) ~2.7 Ma ago yielded 41-kyr cycles of ice sheet advance and retreat (Imbrie et al., 1992) (as distinguishes Milankovitch and Adhémar/Croll theory), but that the dominant ice age period shifted to ~100-kyr cycles of gradual advance and abrupt retreat during the Mid-Pleistocene Transition (MPT) about one million years ago (Imbrie et al., 1993). The difference in phenology of glacial cycles before and after the MPT would require a novel orbital theory, beyond Milankovitch theory, such as skipping of 1 or 2 obliquity maxima (warm polar summers) to yield an average 100- kyr ice age period (Huybers, 2006; Huybers and Wunsch, 2005; Tziperman et al., 2006; Tzedakis et al., 2017; Köhler and Van De Wal, 2020) or non-linear phase locking of climate to the 100- kyr cycle of orbital eccentricity that modulates the intensity of precessional insolation forcing (Pilgrim, 1904; Imbrie et al., 1993; Shackleton, 2000; Maslin and Ridgwell, 2005; Raymo et al., 2006; Lisiecki, 2010; Huybers, 2011; Rial et al., 2013; Barker et al., 2022, 2025; Hobart et al., 2023; Ganopolski, 2024; Zhang et al., 2025). Nodal precession of Earth's orbit also has a 100-kyr periodicity (Fig. 1A right), but it has no direct effect on Earth's orientation toward the Sun (Muller and MacDonald, 1997), and its 100-kyr phase is offset by 30 thousand years from the actual ice age climate cycles, making it an unlikely contributor to the ice ages (Berger, 1999). In contrast to all these orbital theories for 100-kyr ice ages after the MPT, there is also the possibility that the 100-kyr cycle is an intrinsic mode

[4] Milankovitch (1930), p.A143: "During the ice ages [. . .] we need to separate regions as follows: into those outside the glaciation, those in the core of the glaciated area, and those marginal regions at the transition of glaciated and non-glaciated regions. In the non-glaciated region, considering insolation changes even during ice age periods, everything stays as it was during the interglacial period; that is, temperatures change in parallel with [local] insolation. In the other two categories differences arise between changes in insolation: the minima in temperature are amplified, and in the glaciated regions the warming between neighboring minima is weakened [. . .] so that two separate time intervals of cold summer leave behind the impression of one unified ice age."

CLSS: 00056

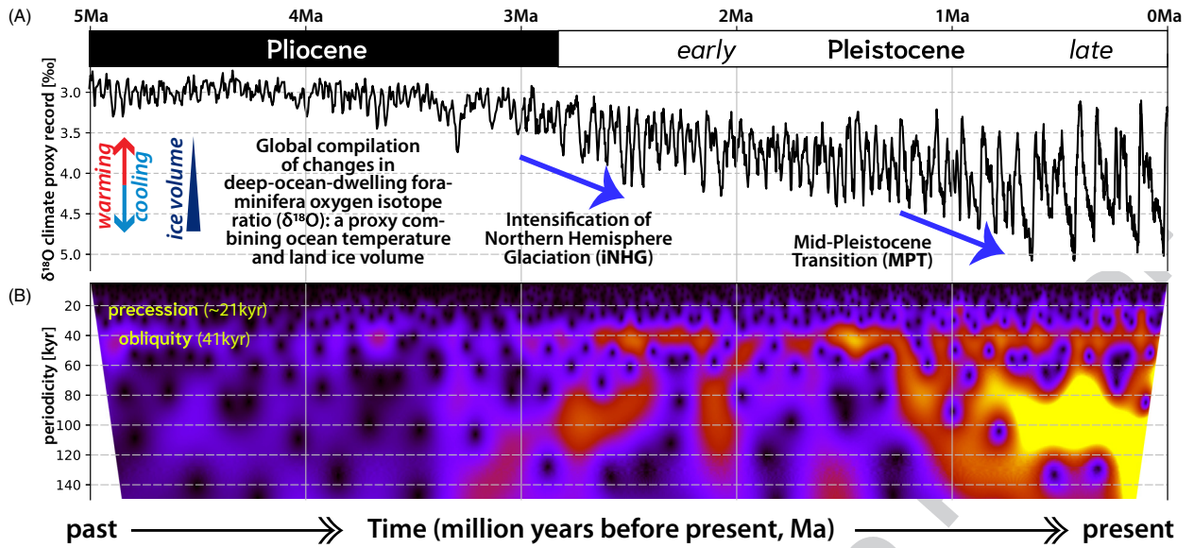

f0015 **Fig. 2** Evolution of "ice age" climate cycles, as reconstructed by the benthic foraminifera oxygen isotope climate proxy that records a combination of temperature and ice sheet changes (Lisiecki and Raymo, 2005). The transition from the Pliocene to the Pleistocene geologic period is characterized by the intensification of Northern Hemisphere Glaciation (iNHG). During the Mid-Pleistocene Transition (MPT), the amplitude and period of cold glacial stages increase, and it is frequently identified as the time when the apparent period of the ice age cycles lengthens from dominantly "obliquity-like" (~41 kyr) to more "eccentricity-like" (~100 kyr). The evolving periodicities of climate variability can be further visualized by continuous wavelet transformation (panel B), where the absence of variability for a given periodicity (y-axis) is shown in black and the warming of colors from blue to red and yellow reflects greater variability at the indicated period. Variability with the 41-kyr period of orbital obliquity is evident throughout the record, but its power increases markedly during the iNHG and remains elevated thereafter. Variability with the ~21-kyr period of precession is much weaker than obliquity throughout the record, but its power increases markedly from the MPT onward. The apparent ~100-kyr variability that developed during the Pleistocene is a key unresolved aspect of the ice age cycles, most often attributed to the eccentricity cycle (Fig. 1A). Additional spectral analysis of the oxygen isotope record is shown in Fig. 6B.

of climate system variability (Saltzman and Maasch, 1988; Shackleton, 2000; Toggweiler, 2008; Riechers et al., 2022; Mitsui et al., 2025; Koepnick and Tziperman, 2024).

s0035 Ice sheet dynamics

p0080 Early records revealed that recent ice ages followed a distinct "sawtooth" pattern of long periods of ice sheet growth and cooling followed by brief periods of deglaciation and warming (Broecker and Van Donk, 1970). Subsequent refinements of the climate record confirmed that this pattern has a ~100-kyr period even though Northern Hemisphere and boreal insolation forcing has little spectral power in the 100-kyr band (Hays et al., 1976; Imbrie et al., 1984). It was hence concluded that the dynamic behavior of the ice sheets integrated orbital forcing (Imbrie and Imbrie, 1980) and that the changes in ice and climate were *paced* but not uniquely *controlled* by insolation change (Imbrie et al., 1993). For example, the idea that ice sheets grow slowly but melt quickly as they follow orbitally-forced changes in ice sheet size was influential, eventhough it did not resolve the glaciologic mechanisms that control the ice sheet response to forcing.

p0085 According to Milankovitch (1930, 1941), northern ice sheets initiate when winter season snowfall exceeds summer season melting, which in the case of mountain glaciers corresponds to the "snowline" above which snow and ice cover persists through the summer melt season. Milankovitch also identified two positive feedbacks that amplify the response of ice sheets to forcing (Fig. 3A), including the ice–albedo feedback (see also Croll, 1875; Manabe and Wetherald, 1975) and the accumulation-elevation feedback (Levermann and Winkelmann, 2016). In the ice–albedo feedback, orbitally-driven reduction in boreal summer insolation causes relatively cool summers that lower the elevation of the snow line and hence permit summer season snow cover. Further, snow and other forms of ice reflect 40–90% of incoming insolation (albedo α of 0.9 and 0.4 for fresh and melting snow, respectively; Gardner and Sharp, 2010) compared to <20% for bare soils, grasslands and forests (α between 0.1 and 0.2; Rechid et al., 2009), resulting in a large potential change in net absorbed insolation ($\triangle F_{net}$):

$$\triangle F_{net} \approx (1-\alpha) * \triangle F_{in} - \triangle\alpha * \overline{F_{in}}$$

p0090 For example, summer solstice daily incoming insolation at 65°N varies between ~450-515 W/m^2 (F_{in}; Huybers, 2006), with a mean of ~480 W/m^2 ($\overline{F_{in}}$) and up to -65 W/m^2 incoming radiative forcing ($\triangle F_{in}$) associated with the change from perihelion to aphelion summer solstices, and with -52 W/m^2 net radiative forcing when assuming a snow-free landscape (α of 0.2; first term on right hand side). Assuming a change to melting but persistent summertime snow cover ($\triangle\alpha$ of 0.2) reduces net orbital insolation forcing to 39 W/m^2 and results in -96 W/m^2 mean albedo forcing (second term). Considering the seasonal energy budget, Milankovitch

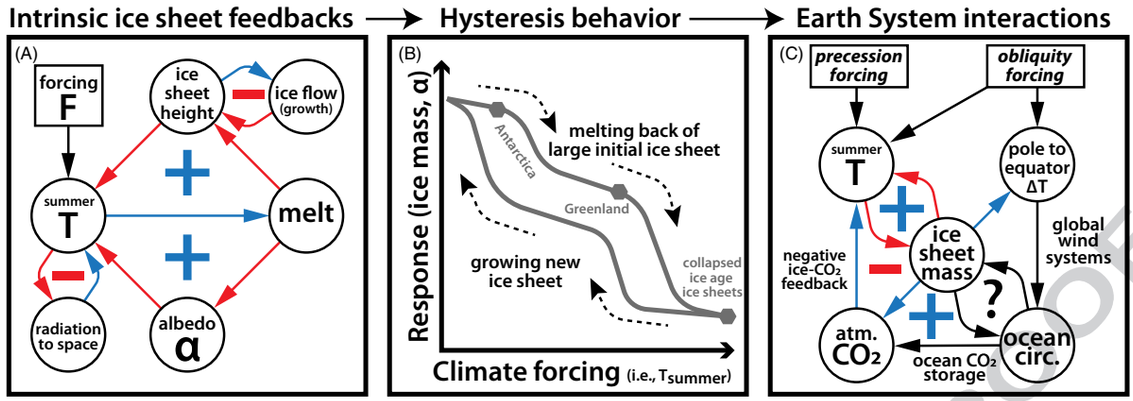

f0020 **Fig. 3** Illustration of the dynamic behavior of ice sheets in the Earth System. (A) Ice sheet mass balance and lateral ice flow is linked to melt-season temperatures, as proposed by Brückner et al. (1925) and Milankovitch (1930). Cold summers lead to less melting and allow year-over-year accumulation of snow that raises surface elevation and landscape albedo (i.e., fraction of incoming sunlight reflected to space, α), both contributing positive (+, i.e., amplifying) feedbacks on summer temperature (i.e., causing additional cooling). In the local energy balance, cool summers yield less upward radiation (to space), thereby stabilizing surface temperatures through a negative (−, i.e., stabilizing) feedback. Likewise, snow only accumulates to the point that snow fields turn into glaciers, which flow and grow laterally, in a negative (stabilizing) feedback on ice surface elevation. These and other feedbacks result in multi-stability and hysteresis behavior of ice sheets (panel B), where the stable size of the ice sheet not only depends on the concurrent summer temperatures but also on the pre-existing state of the ice sheet. In the context of the broader climate system (panel C), the positive ice–albedo feedback also increases the pole-to-equator temperature gradient in the northern hemisphere, which acts to strengthen equator-to-pole heat transport by atmosphere and ocean (Lorenz, 1955; Bryan, 1987; Trenberth, 2022). Further, meltwater input to the polar ocean can disrupt the ocean's overturning circulation (Croll, 1875; Rahmstorf, 1996), with uncertain climate feedbacks with the ice sheets (Snoll et al., 2024). Finally, when ice sheets grow, they withdraw freshwater from the ocean, lowering sea level, reducing the mass of the ocean and thereby leading to persistent CO_2 increase to form a negative (−) feedback (Hain and Sigman, 2024). In contrast, change in the ocean's circulation and its relationship to biological productivity alters CO_2 storage in the ocean's deep water, which is thought to be the primary cause for low atmospheric CO_2 concentration during ice ages, forming a strong positive (+) ocean-CO_2 feedback (see Fig. 5C). Because of the central role of ice sheets in ice age climate change, it seems likely that the broader climate system inherits hysteresis behavior from the ice sheets. Solid arrows represent causal links, with blue indicating that a cause leads to the same sign in its effect while red indicates that a cause leads to the opposite sign in its effect.

estimated about 1 K of regional summer cooling and 60 m of snowline lowering per $-10\ W/m^2$ net radiative forcing,[5] and assuming that the region becomes fully ice covered, he projected that the net radiative forcing would be up to three-times greater than the incoming radiation orbital forcing.[6] Early numerical ice sheet energy balance models encapsulating these feedbacks yielded the insight that if Earth ever became glaciated, it would absorb too little solar radiation and be too cold to melt (Budyko, 1969; Sellers, 1969; Faegre, 1972), presaging the discovery of "snowball Earth" global glaciation events in Earth's deep geologic history (Kirschvink, 1992; Hoffman et al., 1998; Macdonald et al., 2010) and providing the first evidence for the multi-stability and hysteresis behavior of ice sheets.

p0095 Modern process-based ice sheet models retain the classical positive (amplifying) feedbacks of energy balance but have a strong emphasis on the dynamic flow of ice and the diverse effects that govern the continuum mechanics of ice deformation (Greve and Blatter, 2009). This shift away from local energy balance is based on the recognition that even within a stable ice sheet, the ice itself is continuously flowing from high elevation accumulation zones to low-elevation ablation or calving zones. If an ice sheet is frozen solid to crystalline bedrock, the ice flow is relatively slow and entirely accommodated by ice deformation, with frictional heating dispersed throughout the ice column. In contrast, in "wet-based" ice sheets or ice sheets frozen to soft sediment layers, "regolith" friction is relatively low, ice flow is relatively fast and accommodated by sliding at the base or within the regolith (Morland et al., 1984; Piotrowski and Tulaczyk, 1999; Pollard and DeConto, 2012). One prominent hypothesis posits that the erosion of subglacial regolith after the iNHG progressively increased basal friction, causing ice sheets to grow thicker and become more stable (Clark and Pollard, 1998), leading to the larger and longer-lasting ice ages after the MPT (see Fig. 2).

p0100 Current generation ice sheet models suggest that hysteresis is a general characteristic of ice sheets (Pollard and DeConto, 2005; Calov and Ganopolski, 2005; Schoof, 2007; Abe-Ouchi et al., 2013; Ullman et al., 2014; Garbe et al., 2020; Van Breedam et al., 2023; Gutiérrez-González et al., 2025; Leloup et al., 2025). As a key result, growing an ice sheet of a certain size requires a colder climate than is needed to maintain an existing ice sheet (Fig. 3B; e.g., Gutiérrez-González et al., 2025). We know from the ice core record that the Greenland ice sheet was markedly smaller in the previous "Eemian" interglacial climate stage (NEEM community members, 2013), when temperature reconstructions suggest marginally warmer global climate but substantially warmer local climate (Leduc et al., 2010; Capron et al., 2014; Landais et al., 2016). Models suggest that anthropogenic warming could irretrievably destabilize the Greenland ice sheet if regional summer season temperatures exceed a warming threshold of 1-3 K for a protracted period (Fox-Kemper et al., 2021), in this case forced by greenhouse gas emissions rather than the orbital forcing

[5]Milankovitch (1930) equations 48 and 49, p.A168.

[6]Milankovitch (1941) Table XXVIII, comparison of Figure 55 illustrating orbital forcing without ice–albedo feedback and Figure 56 illustrating net radiative forcing of orbit and northern ice sheet albedo.

considered by Milankovitch. In these models, the melting back generally takes thousands of years (Alley et al., 2005) but may proceed in abrupt steps due to additional threshold instabilities, for example, related to the buttressing effect of floating ice shelves (Schoof, 2007) or ice sheet saddle collapse (Gregoire et al., 2012; Reyes et al., 2024). While Milankovitch's focus on melt season temperature is supported by these models, the intrinsic hysteresis behavior of the ice sheets integrates orbital, greenhouse gas and stochastic forcing from weather and climate variability (Fig. 3C).

p0105 Beyond the intrinsic ice sheet behavior in response to forcing, coupled Earth System models of the climate system and ice sheets demonstrate feedbacks between the simulated ice sheets, climate and ocean circulation (Fig. 3C). However, because of the long-timescale response of the ice sheets, model studies typically use computationally efficient idealized models (Ganopolski et al., 2010) and/or idealized experiments with limited coupling between the ice sheets, climate and ocean (Yun et al., 2023), thus potentially underestimating the role of hysteresis in the glacial cycles. Ice sheets' influence on climate can extend beyond regional albedo-driven cooling. For example, ice albedo at high latitudes results in differential heating of the tropics that strengthens atmospheric circulation (Lorenz, 1955), similar to obliquity forcing, but, in the case of waxing and waning boreal ice sheets, mostly affecting the Northern Hemisphere (Fig. 3C). In addition, the implied meltwater released from retreating ice sheets has long been suspected to drive reconstructed changes in the Atlantic Meridional Overturning Circulation (AMOC) (McManus et al., 2004), thereby contributing to reconstructed millennial-scale climate variability, possibly impacting Southern Ocean circulation and, thus, atmospheric CO_2 during glacial terminations (Sigman et al., 2007; Denton et al., 2010). In the following sections we survey key reconstructions and model results that inform our understanding of climate and ice sheet effects on ocean circulation and atmospheric CO_2.

s0040 Ocean circulation

p0110 James Croll originally proposed that ocean circulation participates in orbitally-forced ice age climate cycles by redistributing heat from the tropics to higher latitudes. Croll specifically highlighted the possible cessation of the Gulf Stream as a primary driver of regional climate change and glaciation:

> The enormous extent to which the thermal condition of the globe is affected by ocean-currents seems to cast new light on the mystery of geological climate. What, for example, would be the condition of Europe were the Gulf-stream stopped, and the Atlantic thus deprived of one-fifth of the absolute amount of heat which it is now receiving – Croll (1875) dq0015

p0115 Modern observations and models support Croll's basic argument about the role of ocean circulation and heat transport in the climate system (Trenberth, 2022), with net ocean heat transport from the Southern to the Northern Hemisphere concentrated in the Atlantic. Moreover, reconstructed changes in ocean circulation at the end of the LGM resemble Croll's scenario. From this perspective, Milankovitch's exclusive focus on albedo[7] was a retrenchment from an integrative view of the glacial cycles (e.g., Chamberlin, 1897, 1899; Croll, 1875). However, the role of ocean circulation in the ice age cycles remains unclear. Below, we first summarize key features of modern ocean circulation and then describe reconstructions of past changes in ocean circulation and climate.

p0120 A distinction has been drawn between the fast, wind-driven geostrophic circulation of the upper ocean subtropical gyres (Sverdrup, 1947; Stommel, 1948; Munk, 1950) and the slow overturning circulation of the global deep ocean (Stommel and Arons, 1959; Bolin and Stommel, 1961; Munk, 1966). The upper ocean is responsible for most of the ocean's heat transport (Bryan, 1987), with each ocean basin hosting a warm, poleward-flowing current on the western boundary and an equatorward return flow of relatively cool water in the eastern part of the basin (e.g., Talley, 2011). However, the deep ocean may be important for heat transport between the polar regions of each hemisphere. Moreover, the circulation of the deep ocean is central to the ability of the ocean to store CO_2 by biological means (Sarmiento and Toggweiler, 1984; Toggweiler and Sarmiento, 1985; Siegenthaler and Wenk, 1984; Knox and McElroy, 1984).

p0125 Because deep water ^{14}C ages are relatively young in the North Atlantic and get older toward the deep Pacific, Broecker (1987, 1991) rationalized the ocean's global overturning circulation as a single-loop 'conveyor belt' with new cold deep water formed in the boreal North Atlantic (North Atlantic Deep Water, NADW) that slowly spreads into the global deep ocean, is upwelled to the surface in the Indo-Pacific, where it heats up and is returned as a warm surface current to the boreal North Atlantic (Fig. 4, modern circulation at top). It was later realized that the ocean's global overturning circulation is better described as an overlapping double-loop, with deep water formation in both North Atlantic (NADW) and in the Antarctic Zone of the Southern Ocean (Antarctic Bottom Water, AABW) dynamically balanced by westerly wind-driven upwelling of deep water in the Southern Ocean frontal system (Toggweiler and Samuels, 1995; Kuhlbrodt et al., 2007; Talley, 2013; Fig. 4A).

p0130 The upper overturning cell, often referred to as Atlantic Meridional Overturning Circulation (AMOC), functions to convey heat from the tropics and Southern Hemisphere to the boreal North Atlantic (Bryan, 1987; Kuhlbrodt et al., 2007). If the AMOC were to stall, the associated changes in ocean heat transport would cool the North Atlantic region and differentially heat the Southern Hemisphere (Broecker, 1998; Seidov and Maslin, 2001), much as suggested by Croll. Coupled climate-ocean circulation models suggest that the AMOC strength responds to the freshwater balance of the North Atlantic, with bi-stability and hysteresis behavior

[7] Milankovitch (1930), p.A115 "Calculated and observed temperatures differ [... because] the Theory was forced to disregard the effects of Air and Ocean currents."

CLSS: 00056

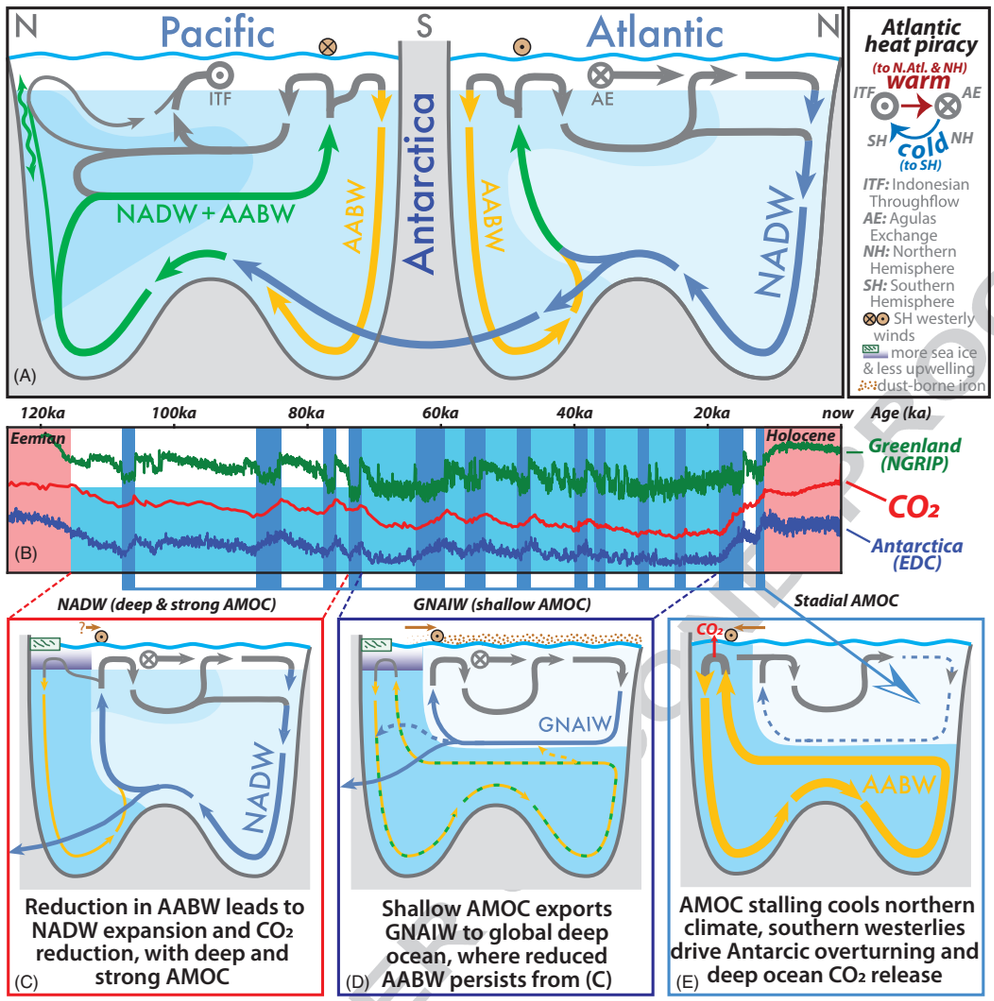

f0025 **Fig. 4** Illustrations of (A) the modern deep ocean overturning circulation, (B) synchronized ice core climate records from Greenland (North Greenland Ice Core Project members, 2004; Capron et al., 2010), Antarctica (EDC, Jouzel et al., 2007) and atmospheric CO_2 (Lüthi et al., 2008), and (C,D,E) different patterns of ocean overturning during the last glacial cycle. The formation and export of North Atlantic Deep Water (NADW, blue) is balanced by other flows. Together, these comprise the Atlantic Meridional Overturning Circulation (AMOC), which transports southern hemisphere heat to the North Atlantic region (i.e., "Atlantic heat piracy" schematic, top right legend). NADW mixes with Antarctic Bottom Water (AABW; yellow) to fill the modern deep ocean (mixture shown in green). This pattern of circulation has prevailed during the current (Holocene) and the previous (Eemian) interglacial periods, which are characterized by minimal northern glaciation and relatively high CO_2 (red shading in B). Over the course of the last ice age cycle, we highlight three patterns of circulation change (Böhm et al., 2015; Sigman et al., 2010, 2003; Hain et al., 2010). (C) First, at the end of the previous interglacial (~110 ka), one interpretation of the available data is that Antarctic overturning and AABW formation declined and remained at a lower level for the rest of the ice age, to strengthening the ocean's biological pump and thus lower atmospheric CO_2 (Hain et al., 2010; Studer et al., 2015). An alternative view is that, regardless of Antarctic overturning rate, sea ice cover prevented CO_2 escape from the Antarctic surface to the atmosphere (Stephens and Keeling, 2000; Marzocchi and Jansen, 2019). (D) Second, during the penultimate obliquity minimum (since 70 ka), the AMOC shoaled, yielding a shallower form of NADW that is often referred to as Glacial North Atlantic Intermediate Water (GNAIW). This mode of Atlantic circulation apparently continued to import Southern Hemisphere heat to the North Atlantic region and to export cold subsurface water to the global ocean—perhaps still mixing with AABW (dashed green; Hain et al., 2010; Kwon et al., 2012) and thereby contributing to reduced atmospheric CO_2 at this time. In addition to this circulation change, data suggest that iron fertilization of phytoplankton in the Subantarctic region of the Southern Ocean strengthened ocean CO_2 storage, also working to lower atmospheric CO_2 in the later, deeper part of the ice age (Martínez-García et al., 2014). (E) Third, millennial-scale cold ("stadial") events in the North Atlantic region (and Northern Hemisphere broadly) occurred throughout the last glacial cycle, independent of orbital forcing. These events were associated with reduced NADW formation and lower AMOC-driven heat import to the North Atlantic. The strongest and longest of these events (dark blue shaded intervals) were consistently associated with Southern Hemisphere warming and atmospheric CO_2 increase (Ahn and Brook, 2008). Modes (C) and (D) are hence related to the build-up of ice ages, while the millennial mode (E) is implicated in the termination of the last ice age and of other late Pleistocene terminations (McManus et al., 2004; Sigman et al., 2007; Denton et al., 2010; Rafter et al., 2022).

that lead to abrupt boreal climate change in response to gradual freshwater forcing (Manabe and Stouffer, 1988; Rahmstorf, 1995, 1996). In the context of future climate, this could mean that the AMOC is on the verge of shutdown as various sources of freshwater to the North Atlantic increase under anthropogenic forcing (Ditlevsen and Ditlevsen, 2023; Drijfhout et al., 2025), with the caveat that the continued wind-driven upwelling of dense waters in the Southern Ocean and continued northward heat transport of the North Atlantic subtropical gyre may sustain the AMOC for this century or longer (Baker et al., 2025). In the context of Quaternary climate history, there is striking evidence for 'violent shifts' in Greenland temperatures during the last glacial cycle (Dansgaard et al., 1982, 1984, 1993; Johnsen et al., 1992; North Greenland Ice Core Project members, 2004) (Fig. 4B,E) and cold 'stadial' periods of extensive ice-rafted debris in North Atlantic sediments (Heinrich, 1988; Hodell et al., 2008) that correlate with Antarctic warming (Barker et al., 2009; Capron et al., 2010) and shifts in tropical hydro-climate (Haug et al., 2001; Peterson et al., 2000; Wang et al., 2001, 2005, 2008; Chiang and Koutavas, 2004; Broecker, 2006). Reduced AMOC heat transport may have promoted Eurasian ice sheet growth before the Last Glacial Maximum (Liu et al., 2025; Niu et al., 2024). As such, the dynamic behavior of the AMOC appears to be the leading cause of millennial-timescale spectral power in the Quaternary climate record (Barker et al., 2011). It remains unclear how the dynamic behavior of the AMOC interacted with the dynamic freshwater balance of the northern ice sheets (Snoll et al., 2024), but it is clear that cold climate conditions (Barker et al., 2009; Hodell et al., 2017) and reduced NADW production (Robinson et al., 2005; Thornalley et al., 2011; Fig. 4E) persisted for almost 3000 years (17.5 to 14.6 ka) before giving way to abrupt warming (Clark et al., 2012) and protracted ice sheet melt-back (Deschamps et al., 2012). That is, the vast northern ice sheets that had grown during optimal orbital conditions at 21 ka ago (low obliquity, northern summer solstice during aphelion) maintained their ice volume under deteriorating orbital forcing until AMOC heat transport commenced at 14.6 ka, after which time the northern ice sheets rapidly melted back (Peltier, 2005). Given the orbital periodicities of the glacial cycles, many investigators believe that the collapse of the ice sheets is primarily determined by orbital forcing that triggered AMOC change (e.g., Denton et al., 2010).

p0135 An additional focus of attention is the response of the "lower cell" of ocean overturning to orbital forcing, "upper cell" AMOC variability, and the ice sheets. When forced with ice age climate conditions, early coupled ocean-climate models reduced deep ocean overturning under sea ice cover of the polar ocean (Manabe and Bryan, 1985). However, simulations with more recent models instead tend to form deepwater during sea ice production and thereby accelerate the lower cell under cooler climates (Otto-Bliesner et al., 2007). With these models, simulations of colder climate (e.g., the Last Glacial Maximum, LGM) tend to yield a shallower AMOC and a lower overturning cell that is expanded under the influence of Antarctic sea ice formation and export (Manabe and Stouffer, 1999; Ferrari et al., 2014; Jansen, 2016). This AMOC response appears consistent with the paleoceanographic observations, which suggest a shift from the North Atlantic Deep Water of today to "Glacial North Atlantic Intermediate Water" during the LGM and previous ice ages (Duplessy et al., 1988; Curry and Oppo, 2005; Lynch-Stieglitz et al., 2007; Fig. 4D). This tendency to enhance lower cell overturning also arises when ocean models are forced with LGM obliquity and greenhouse gas concentrations (Timmermann et al., 2007; Galbraith and De Lavergne, 2019; Yun et al., 2023).

p0140 While it is reasonable to assume that the more recent generations of climate ocean models most accurately project ocean circulation change under ice age conditions, it is worth pointing out that these same models struggle to capture key aspects of the modern ocean (Donohoe et al., 2024; Chen et al., 2025). There is particular concern that ocean circulation models tend to form new AABW by open Antarctic deep convection (e.g., Killworth, 1983; Jansen, 2017; Marzocchi and Jansen, 2019), whereas AABW formation and deep cell ventilation appear to dominantly involve other oceanographic processes ((Broecker et al., 1985); Gebbie and Huybers, 2010; DeVries and Primeau, 2011; Rae and Broecker, 2018; Abernathey and Ferreira, 2015; (Orsi et al., 2002)). This has implications for CO_2 storage in the ocean (Hain et al., 2010; Kwon et al., 2012; Sigman et al., 2021), which is the central topic of the next section.

s0045 Atmospheric carbon dioxide

p0145 The sensitivity of Earth's climate to the atmospheric trace gas carbon dioxide (CO_2) first arose from experiments that showed certain "green-house gases" (GHGs; water vapor, CO_2, methane, nitrous oxide) absorb infrared radiation (Fourier, 1822; Pouillet, 1827, 1838; Foote, 1856; Tyndall, 1860). Svante Arrhenius (1896) quantified the CO_2 effect on surface temperature based on the observed atmospheric absorption spectrum of infrared moonlight (Langley, 1890). In his calculations, Arrhenius assumed that the water vapor content of air changed so as to maintain constant relative humidity. That is, he included a positive water vapor feedback that increases the sensitivity of equilibrium surface temperature to CO_2 forcing, with the core result that Earth's global mean temperature (GMT) would need to warm by about 3 K for every 50% increase of CO_2 ($\triangle \log_{1.5} CO_2$) to maintain radiative energy balance with space—equating to about 5.1 K per CO_2 doubling ($\triangle \log_2 CO_2$):

$$\triangle GMT_{Arrhenius} = 3K \cdot \triangle \log_{1.5} CO_2 = 5.1K \cdot \triangle \log_2 CO_2$$

p0150 This fundamental logarithmic relationship between quasi-global temperature change ($\triangle$GMT) and CO_2 doublings ($\triangle \log_2 CO_2$) was questioned by Milankovitch[8] but ultimately reconfirmed in the discovery of anthropogenic warming (Callendar, 1938,

[8] Milankovitch *(1941), p. 448:"Because the carbonic acid [CO_2] content of the atmosphere [. . .] is less than 0.03% [<300 ppm], I will treat dry air as homogenous gas and only include the special role of water vapor.";* Milankovitch *(1941) p.451:* "L. de Marchi and Arrhenius have based their ice age theories on the influence of water vapor and carbonic acid [CO_2] on the absorption of outgoing [thermal] radiation. I have discussed both their theories [in Milankovitch, 1920], and clarified the reasons for their inadequacy."

Callendar, 1949). Subsequently, the concept of Equilibrium Climate Sensitivity (ECS; the global mean temperature increase per doubling of atmospheric CO_2, i.e., $\triangle GMT/\triangle \log_2 CO_2$) became a core principle of climate science (Charney et al., 1979). ECS relates the radiative forcing from CO_2 change (F_{CO2}) to the change of Earth's radiation to space in response to $\triangle GMT$ (R_{GMT}). In this framework of radiative surface temperature regulation, forced warming (positive F, positive $\triangle GMT$) leads to more outgoing radiation (negative R), thereby establishing a negative radiative "climate feedback" that restores radiative balance ($\delta Q/\delta t = 0$, where Q can be thought of as the energy in the Earth System) with a certain amount of equilibrium warming ($\triangle GMT_{eq.}$) per CO_2 forcing (F_{CO2}):

$$\frac{\delta Q}{\delta t} = F_{CO_2} + R_{GMT} = 3.7\frac{W}{m^2} \cdot \triangle \log_2 CO_2 + \Sigma\lambda_{ECS} \cdot \triangle GMT_{eq.} = 0$$

$$ECS = \frac{\triangle GMT_{eq.}}{\triangle \log_2 CO_2} = \frac{-3.7\frac{W}{m^2}}{\Sigma\lambda_{ECS}}$$

p0155 One doubling of CO_2 ($\triangle \log_2 CO_2$) causes +3.7 W/m^2 radiative forcing (F_{CO2}), while 1 K of warming is thought to increase outgoing radiation by about 1.3 W/m^2 (negative R_{GMT}, $\Sigma\lambda_{ECS}$ of about −1.3 W/m^2/K), leading to an estimate for ECS between 2.3 and 4.5 K equilibrium warming per CO_2-doubling (Sherwood et al., 2020). In this physical interpretation, ECS results from the sum of multiple individual feedbacks (Fig. 5A), dominated by the negative Planck radiative feedback (higher temperature resulting in more infrared radiation to space) that is critical to establish radiative balance (−3.2 W/m^2/K). Most other climate feedbacks contributing to ECS are positive, increasing Earth's equilibrium temperature response to radiative forcing: With rising GMT, the combined effect of the positive water vapor feedback and a net-negative lapse-rate feedback is to block more outgoing radiation (+1.2 W/m^2/K), while the effects of clouds and land-surface albedo cause further positive radiative feedbacks (of +0.45 W/m^2/K and + 0.3 W/m^2/K, respectively). All of these feedbacks are fast-acting and thus relevant to ongoing global warming: Currently, the heating rate $\delta Q/\delta t$ and F + R are roughly +1 W/m^2.

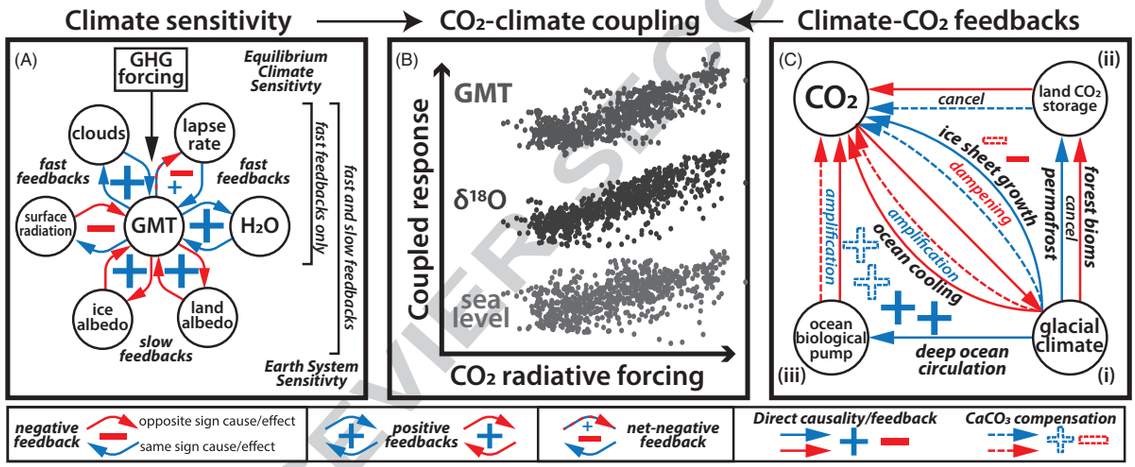

f0030 **Fig. 5** Illustration of (A) the key feedbacks determining the Global Mean Temperature (GMT) change and Earth's net radiative response to radiative forcing, (B) the reconstructed correlation between CO_2 radiative forcing climate variables over the last 800 kyr, and (C) the carbon cycle feedback dynamics that naturally regulate climate and CO_2. In the context of the ongoing anthropogenic greenhouse gas (GHG) forcing that is driving global warming, the negative (−) Planck-feedback to warming is an increase in upward surface radiation that functions to stabilize surface temperature. However, the net radiative response also includes fast-acting net positive (+) feedbacks from the atmosphere's water vapor, lapse rate and clouds, all of which contribute to Equilibrium Climate Sensitivity (ECS): the GMT increase needed to balance a given radiative forcing (see Sherwood et al., 2020). On longer timescales and in the context of the ice ages, slow-acting positive (+) albedo feedbacks of the land surface, the ice sheets and atmospheric dustiness further amplify the GMT change needed to re-establish radiative balance per given increment of GHG forcing (in the case of an ice age, a GMT decrease in response to a negative GHG forcing). The combined effects of albedo and CO_2 forcing appear necessary and sufficient to explain observed global cooling during the Last Glacial Maximum (Zhu and Poulsen, 2021; Yun et al., 2023; Tierney et al., 2020; Hain and Sigman, 2024). However, the CO_2 effects of physical ice age changes (ice sheet growth, sea-level lowering and ocean cooling, labeled (i) in panel C) largely cancel one another on the timescale of ocean overturning (solid arrows from climate to CO_2 in panel C) and on the timescale of ocean carbonate compensation (dashed arrows from climate to CO_2 in panel C). Moreover, ice age increases in permafrost and land biome carbon storage apparently canceled as well, and the residual effect on atmospheric CO_2 from net loss in land carbon would have been canceled by ocean uptake and carbonate compensation (right and top in panel C labeled (ii); Hain and Sigman, 2024)—as will be the fate of CO_2 emitted by human activities (Archer et al., 2009). In contrast, enhanced biological carbon storage in the deep ocean (labeled (iii) in panel C) directly lowers CO_2, and this effect is amplified by carbonate compensation (Hain et al., 2010). Thus, it appears that coupled changes in the ocean's circulation and biological pump are the primary cause of ice age reduction in atmospheric CO_2. In turn, CO_2 radiative forcing explains a large portion of the reconstructed ice age global cooling (panel B). The legend distinguishes negative and positive feedbacks (+,−) and highlights intermediate cases where the feedback dynamic has positive and negative aspects, i.e., the lapse rate feedback is net-negative globally but positive in polar regions, or the net-positive climate CO_2 feedbacks of panel C.

p0160 On the long timescale of ice ages, additional feedbacks arise. Evidence suggests that the positive ice–albedo feedback (–3 W/m^2 at –5 K during the Last Glacial Maximum; Köhler et al., 2010), and the positive dust–albedo feedback further increased the sensitivity of GMT to CO_2 radiative forcing, the long-term Earth System Sensitivity (ESS, Fig. 5A; Rohling et al., 2018):

$$ESS = \frac{-3.7\,\frac{W}{m^2}}{\Sigma\lambda_{ECS} + \lambda_{ice-sheets} + \lambda_{dust} + \ldots}$$

p0165 Arrhenius (1896) thus hypothesized that evidence for past climate change can be explained by changes in atmospheric CO_2 and subsequent climate feedbacks.

p0170 Arrhenius could only speculate as to if and why CO_2 might have changed in the past. It was only in the late 20th century that glaciologists began to recover Antarctic ice cores dating back to the Last Glacial Maximum (LGM) for the purpose of reconstructing past atmospheric CO_2 concentrations from the trapped air bubbles. From that work we learned that CO_2 concentrations were roughly a third lower during the LGM (Delmas et al., 1980; Neftel et al., 1982; Raynaud et al., 1982; Stauffer et al., 1984; Raynaud and Barnola, 1985). Continued ice-coring in Antarctica and the development of analytical methods for ice core analysis has ultimately yielded a continuous CO_2 record for the last 800 thousand years (Barnola et al., 1987; Petit et al., 1999; Siegenthaler et al., 2005; Lüthi et al., 2008; Bereiter et al., 2015), demonstrating a very strong correlation between atmospheric CO_2 radiative forcing and the records of glacial/interglacial climate change (Fig. 5B). Remarkably, the climate-CO_2 relationship is stable across major ice age cycles (Siegenthaler et al., 2005), CO_2 radiative forcing is a much better predictor of reconstructed global mean temperature than boreal summer insolation (Fig. 5B), and climate models require CO_2 radiative forcing to reproduce reconstructed ice age global cooling (Zhu and Poulsen, 2021; Yun et al., 2023).

p0175 The ice age CO_2 problem refers to the longstanding challenge to attribute the observed CO_2 changes to physical, chemical, biological and geological driving factors. Mean ocean cooling raises seawater CO_2 solubility and hence lowers atmospheric CO_2, whereas ice sheet growth withdraws water from the ocean (lower sea level; Fig. 5B) and thereby reduces seawater CO_2 solubility and raises CO_2. These direct climate-CO_2 feedbacks, labeled (i) in Fig. 5C, operate on the ocean overturning timescale and are thus fast relative to orbital forcing. Ocean cooling and ice sheet growth also have effects on the solubility of $CaCO_3$ on the deep ocean seafloor, thereby driving a "carbonate compensation" feedback via the ocean's alkalinity budget (dashed arrows in Fig. 5C; Broecker and Peng, 1987; Hain and Sigman, 2024) that is slow relative to climate feedbacks but still faster than orbital forcing. In part because their effects oppose and largely cancel one another, the coupled changes in ocean temperature and ice sheets have minimal net effect on the solubilities of CO_2 and $CaCO_3$, and they thus fail to explain the observed CO_2 changes (Broecker, 1982a, 1982b; Genthon et al., 1987; Hain and Sigman, 2024). Biological carbon storage in terrestrial ecosystems is also directly influenced by climate, labeled (ii) in Fig. 5C, with ice age evidence that forest biomes contracted (Shackleton, 1977; Prentice et al., 1993; Lindgren et al., 2018) while permafrost carbon storage expanded (Crichton et al., 2016; Köhler et al., 2010; Winterfeld et al., 2018); apparently, the net effect was a loss of land carbon storage during the LGM (Peterson et al., 2014; Jeltsch-Thömmes et al., 2019). Such a reduction in land carbon storage would directly raise atmospheric CO_2, but it also lowers the pH and $CaCO_3$ saturation of the ocean, which causes the ocean's carbonate compensation feedback to raise ocean alkalinity, lower atmospheric CO_2, and thereby offset the direct CO_2 effect. That is, land carbon storage apparently acted as a short-term negative climate-CO_2 feedback, but the associated carbonate compensation (as well as the ocean's capacity for dissolved inorganic carbon (DIC) storage even without alkalinity change) caused land carbon storage changes to have only a weak net effect on CO_2 on orbital forcing timescales (labeled (ii) in Fig. 5C). Similarly, the proposal that dissolved organic matter (DOM) accumulated in the ocean during ice ages so as to lower atmospheric CO_2 (Jiao et al., 2010) is largely nullified by the ocean's DIC capacity and the $CaCO_3$ compensation feedback (not shown in Fig. 5C).

p9000 Most biologically-driven reduction in atmospheric CO_2 is achieved by the "biological pump" (Hain et al., 2014), where organic carbon produced by surface ocean plankton sinks to depth before being respired and dissolved back into seawater ("remineralized") in the form of DIC. The biological pump also sequesters in the ocean interior nutrients that are eventually returned to the surface by the ocean's overturning circulation, feeding back into the biogeochemical cycle of plankton growth, sinking, remineralization, and upwelling. Paleoceanographic reconstructions suggest the deep ocean was depleted in oxygen during the ice ages (François et al., 1997; Anderson et al., 2019; Chang et al., 2023; Hoogakker et al., 2018; Jacobel et al., 2020), supporting the hypothesis that ice age CO_2 was lower because carbon storage by the biological pump was significantly greater (Broecker, 1982a, 1982b; Vollmer et al., 2022). Moreover, to the degree that respired carbon storage was concentrated in the deep ocean, it would have increased $CaCO_3$ dissolution off the seafloor to raise ocean alkalinity and further lower CO_2 through a positive carbonate compensation feedback (Boyle, 1988; Sigman et al., 1998; Toggweiler, 1999; Hain et al., 2010; Hain and Sigman, 2024). That is, climate-forced changes in ocean circulation likely induced changes in the biological pump that directly and indirectly lowered CO_2, yielding a strongly positive net climate-CO_2 feedback that persisted on orbital timescales (labeled (iii) in Fig. 5C). For that reason, ice age changes in the biological pump are likely the dominant cause for the reconstructed ice age cycles in atmospheric CO_2 (Hain and Sigman, 2024).

p0180 The Southern Ocean plays a central role in the physical circulation and dissolved chemistry of the deep ocean and has emerged as the key region mediating the efficiency of carbon storage by the biological pump (Sarmiento and Toggweiler, 1984; Toggweiler and Sarmiento, 1985; Siegenthaler and Wenk, 1984; Knox and McElroy, 1984; Sigman and Boyle, 2000; Sigman et al., 2010; Watson et al., 2006). Surface nutrient consumption in the modern Southern Ocean is low (inefficient), and reconstructions suggest it was higher during ice ages (Sigman et al., 2021; references therein). A distinction must be drawn between the Polar Frontal and

Subantarctic Zones (PFZ and SAZ), where surface waters feed into the upper ocean AMOC overturning, and the more polar Antarctic Zone (AZ), where bottom water production feeds into the lower cell of ocean overturning (Fig. 4). In the SAZ, there is clear evidence for dust-borne iron fertilization of phytoplankton growth, carbon export and surface nutrient drawdown during the LGM (Kumar et al., 1995; Martínez-García et al., 2014). In contrast, phytoplankton carbon export in the PFZ and AZ was lower during ice ages (e.g., Jaccard et al., 2013), even as proxy evidence suggests more complete surface nutrient consumption (e.g., François et al., 1997; Ai et al., 2020). Changes in sea ice formation (Ferrari et al., 2014) and westerly wind stress (Toggweiler and Samuels, 1995) are key factors governing Southern Ocean circulation and deep overturning, and sea ice cover can impede CO_2 exchange between the AZ and the atmosphere (Stephens and Keeling, 2000). Debate continues as to the relative importance of ocean circulation and biological productivity versus sea ice-driven air-sea CO_2 exchange limitation in keeping biological pump CO_2 sequestered in the ocean during ice ages (e.g., Sigman et al., 2021; Marzocchi and Jansen, 2019; Khatiwala et al., 2019). From a geochemical perspective, the question can be framed simply as whether the barrier that prevented CO_2 leakage from the Southern Ocean existed at the interface between the surface ocean and the underlying deep ocean, or at the air-sea interface (Archer et al., 2003). This uncertainty aside, there is growing (but not universal) agreement that the Southern Ocean was central to sequestration of CO_2 in the deep ocean during ice ages (Vollmer et al., 2022; Sigman and Hain, 2024).

p0185 The coupled climate-carbon cycle dynamics underlying the ice age cycles have been investigated through the relative timing of events associated with the termination of the Last Glacial Maximum. Boreal summer insolation was at a minimum 21 thousand years ago (ka). Atmospheric CO_2 remained low (Monnin et al., 2001; Marcott et al., 2014) and ice sheets held steady (Deschamps et al., 2012) as orbital forcing became more favorable to deglaciation, according to Milankovitch. Along with Southern Hemisphere warming after 19 ka (Shakun et al., 2012), there is evidence for a reduction in Southern Ocean iron fertilization at the time (Martínez-García et al., 2014), and both of these early deglacial changes implicate the Southern Ocean for the onset of CO_2 rise. Abrupt cooling occurred in the high-latitude Northern Hemisphere (and especially Europe) at ~17.5 ka (e.g., Hodell et al., 2017), most likely caused by reduced AMOC heat transport (e.g., McManus et al., 2004). This cooling was accompanied by Southern Hemisphere warming (Shakun et al., 2012), reduced dust fluxes to the Southern Ocean (Martínez-García et al., 2014), strengthening and southward displacement of the southern westerly winds (Gray et al., 2018; Hall et al., 2026), enhanced wind-driven upwelling in the Southern Ocean (Anderson et al., 2009; Sigman and Boyle, 2000; Toggweiler et al., 2006), and higher concentrations of unused nutrients in the AZ surface (Studer et al., 2015; Wang et al., 2017; Ai et al., 2020), thereby causing ocean CO_2 release to the atmosphere (Rae et al., 2018). By 14.6 ka, orbital forcing was approaching the peak conditions of Milankovitch's preferred deglacial configuration (a substantial maximum in boreal summer insolation), CO_2 had risen by 21% (+1 W/m^2 CO_2 radiative forcing; Etminan et al., 2016), and renewed AMOC heat transport led to abrupt Northern Hemisphere warming (again, especially in Europe; Naughton et al., 2023). It is only at this point that the combined forcing of AMOC, CO_2, and orbit destabilized the Northern Hemisphere ice sheets adequately to terminate the last ice age. This combination of AMOC, CO_2, and orbital forcing seems to have operated in a very similar way during the termination of previous ice ages (Cheng et al., 2009), suggesting a fundamental role for North Atlantic freshwater discharge in deglaciations, perhaps through Southern Ocean changes and their effects on atmospheric CO_2 (Sigman et al., 2007; Denton et al., 2010).

s0050 Chaos and memory in Earth's climate

p0190 Edward Lorenz advanced climate science by demonstrating that *weather* behaves chaotically (Lorenz, 1963). He further suggested that the *climate* of Earth is best described as the statistics of simulated weather (Lorenz, 1964), and, in a clear challenge to Milankovitch theory, he proposed that the climate system need not be deterministic (Lorenz, 1968; for modern appraisal, see Crucifix, 2013). For clarity, in this new statistical climatology, the flap of a butterfly may lead to a tornado or possibly an ice age, where the butterfly is neither sufficient nor necessary for either tornados or ice ages.

p0195 Stochastic climate models can be rationalized in terms of a climate system variable (V) that integrates random "weather noise" (W), where the value of the variable at a given time t (V_t) depends both on its previous value (V_{t-1}) and the added random fluctuation (Hasselmann, 1976):

$$V_t = V_{t-1} + W_t = \sum_{t=0}^{-\infty} W_t$$

p0200 In this simplest case, V will go up and down over time even if W has a mean of zero, and, less intuitively, the variability of V increases over time following the Fokker-Planck equation of Brownian motion (Wiener, 1923; which assumes stationarity, Storch and Zwiers, 1999). Taking the example of a random walk, after a few steps in random directions we can expect to still be in the vicinity of the starting point; however, the more steps we take, the further away we may find ourselves, as a matter of probability. That is, normally distributed random numbers have a flat "white noise" power spectrum (Fig. 6A), but simply taking the cumulative sum of the same white noise will yield a record with a "red noise" power spectrum that increases indefinitely for longer periods of variability (Hasselmann, 1976; Fig. 6A right). The key difference between white and red noise is that subsequent random numbers (W) are independent from each other whereas each random fluctuation (W_t) counts indefinitely toward the evolving cumulative sum—the summation from vantage time $t = 0$ to infinite negative time, that is, the past. In contrast, including a negative feedback acting to restore V to its mean state over a timescale (τ) limits the growth of red noise variability (Hasselmann, 1976):

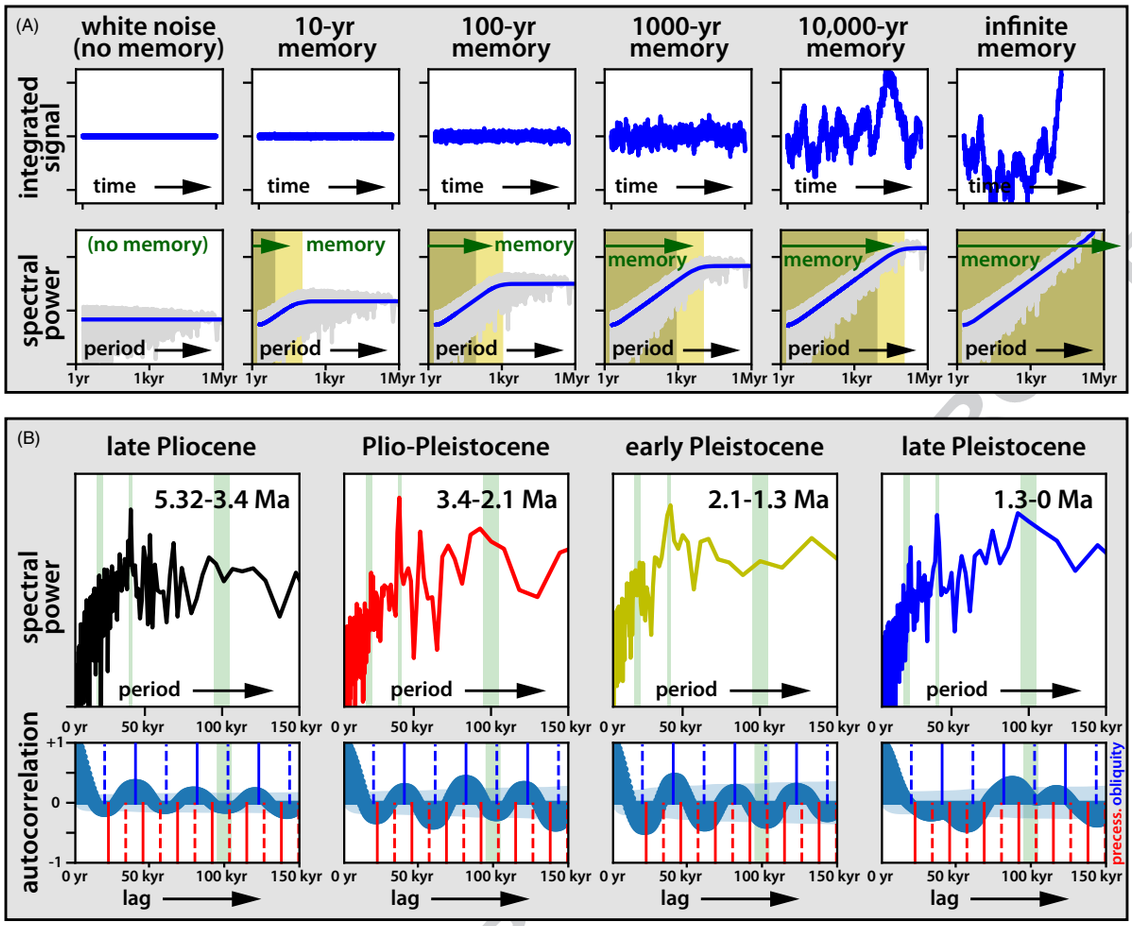

f0035 **Fig. 6** "Climate memory" as a possible contributor to the glacial cycles. (panel A) Slow-acting (negative) stabilizing feedbacks allow short-term random weather fluctuations to accumulate climate variability with longer time-scales. For example, integrating random "white noise" weather with restoring feedback that has an e-folding "memory timescale" yields a power density spectrum of climate variability that rises for periods up to the memory and then plateaus for longer periods. Although the resulting "red noise" is stochastically forced, it represents real changes in climate and hence can trigger additional Earth System feedbacks as well as push across climate thresholds. Inspection of different time slices (B) of the deep-ocean oxygen isotope record (see Fig. 2; Lisiecki and Raymo, 2005) reveals continuum power spectra of climate variability that resemble red noise with a memory of about ~10 thousand years, but including the characteristic spectral peaks corresponding to precession and obliquity (Fig. 1C). Inspection of the autocorrelation for the three intervals of time before the Mid-Pleistocene Transition (left three panels in B) reveals positive correlation persisting for millennial-timescale lags (memory) and regular obliquity oscillation (i.e., with ~41-kyr cyclicity), the dominant orbital forcing. After the Mid-Pleistocene Transition (right panels in B), millennial-scale memory of the climate system persists, spectral density for ~100-kyr periods eclipses spectral density in the obliquity band, and the long-term autocorrelation becomes irregular. The memory of deep ocean circulation is limited by the multi-centennial timescale of ocean overturning, whereas ice sheets and possibly also atmospheric CO_2 contribute memory on multi-millennial timescales.

$$V_t = e^{(-1/\tau)\cdot V_{t-1} + W_t} \approx \sum_{t=0}^{-2\tau} e^{\left(\frac{t}{\tau}\right)} \cdot W_t$$

p0205 The physical interpretation is that the e-folding term relaxes V back to its climatologic mean state while being continuously perturbed by W, and algebraically this also means that V is progressively losing its *memory* of past perturbations beyond about twice its intrinsic e-folding memory timescale (τ, tau). When considering variability with periods shorter than tau, the presence of memory allows random fluctuations to accumulate long-period "red noise" spectral power (khaki shading in Fig. 6), but that increase in spectral power slows for periods greater than tau (light khaki in Fig. 6), and it levels off to yield a flat "white noise" power spectrum for periods about 10 times longer than tau. Hasselmann recognized that the atmosphere has very short-term memory and hence produces short-term "weather noise" (W), whereas the enormous sensible (and latent) heat capacity of the ocean and ice sheets yields long memory in the climate system and thereby increases the absolute level of spectral power of long-period variability. That is, the memory of the ocean and ice sheets integrates weather (short term) variability into longer-term modes of climate variability with progressively greater spectral power (Frankignoul and Hasselmann, 1977; Ghil et al., 2002). For example, integrating annual white noise with a 10-kyr memory timescale (Fig. 6A) produces a continuous "red noise" power spectrum similar to the late Pleistocene climate record, although that red noise lacks the distinct peaks at ~21 kyr, ~41 kyr and ~ 100 kyr

identified in the paleoclimate record (Hays et al., 1976; Imbrie et al., 1984; Fig. 6 gray spectrum). While we present an overly simple example with just one memory term (i.e., one negative feedback), current-generation climate models reveal that physical dynamics in specific regions contribute distinct time-patterns of natural variability (Monselesan et al., 2015; Ghil and Lucarini, 2020), with inter-annual to inter-decadal autocorrelation and modes of variability resulting from the memory of the upper ocean concentrated in the tropics and mid-latitudes, whereas centennial to multi-centennial variability resulting from the memory of the deep ocean is concentrated in the polar ocean surface. The ice sheets and the global carbon cycle contribute memory on millennial and longer timescales. Indeed, if the current Greenland ice sheet wouldn't grow under current climate (i.e., due to ice sheet hysteresis, Fig. 3B) it can be understood as the physical embodiment of climate memory from the last ice age. As such, orbital forcing of the climate mean state would lead to a response that is delayed by the memory of the climate system (Imbrie and Imbrie, 1980; Imbrie et al., 1984), and both orbital and stochastic forcing accumulate power when integrated over the long memories of the ocean, carbon cycle and ice sheets.

p0210 The outstanding challenge with ice age climate change is to accurately attribute the reconstructed spectrum of climate variability to modes of either stochastic internal variability, orbital forcing, geologic forcing, or some combination, and to identify additional mechanisms for the observed changes in spectrum, especially at the intensification of Northern Hemisphere Glaciation ~2.7 million years ago and the Mid-Pleistocene Transition about 1 million years ago (iNHG, MPT in Fig. 2). A linear climate response to obliquity forcing plausibly explains the ~40- kyr cyclicity of early Pleistocene glacial/interglacial cycles (Imbrie et al., 1992), and there are now multiple lines of evidence and models suggesting that the Late Pleistocene ~100-kyr ice age cycles were also a deterministic response to orbital forcing (Raymo, 1997; Raymo et al., 2006; Tzedakis et al., 2017; Willeit et al., 2019; Barker et al., 2025; Hobart et al., 2023; Ganopolski, 2024). Indeed, detailed studies of deep sea records and cave deposits suggest that the timing of glacial terminations is statistically related to obliquity (Huybers and Wunsch, 2005) and to the 100 -kyr eccentricity modulation of precession of the equinox insolation forcing (Imbrie et al., 1993; Raymo, 1997; Ridgwell et al., 1999; Raymo et al., 2006; Huybers, 2006, 2011; Lisiecki, 2010; Parrenin and Paillard, 2012; Abe-Ouchi et al., 2013; Barker et al., 2022; Hobart et al., 2023; Ganopolski, 2024). It is not clear if orbital forcing causes millennial timescale variability (Huybers and Curry, 2006) or if the latter primarily results from stochastic variability in the Atlantic Meridional Overturning Circulation (Barker et al., 2011; Riechers et al., 2022; Stocker and Johnsen, 2003). That is, orbitally forced ice sheet meltwater may have forced millennial-timescale variability in ocean circulation (Denton et al., 2010), or inherent stochastic variability in ocean circulation may have been the primary driver of ice sheet melting (e.g., Deschamps et al., 2012; Piccione et al., 2022). Therefore, it is also unclear if atmospheric CO_2 changes acted as a deterministic feedback amplifying the dynamic response of northern ice sheets to northern summer insolation in line with Milankovitch's hypothesis (e.g., Imbrie and Imbrie, 1986; Raymo et al., 2006), if reconstructed CO_2 radiative forcing of global climate responded primarily to ocean changes (Hain and Sigman, 2024) that emerged largely from orbital forcing but with some role for stochasticity, or if stochasticity was more important than has so far been imagined.

s0055 Perspective

p0215 In the quest to explain the ice age cycles, orbital controls on sunlight have been central from the beginning (Esmark, 1824; Adhémar, 1842). However, the early theorists also considered or included many other aspects of the climate system, including the circulations of atmosphere and ocean (Croll, 1875) and the role of greenhouse gases, CO_2 in particular (Arrhenius, 1896; Chamberlin, 1897). In this regard, an exclusive focus on the work of Milutin Milankovitch (1920, 1930, 1941) as the origin of ice age theory runs the risk of driving an artificial surpremacy of orbital changes and the ice–albedo feedback in explanations for the ice ages. The paleoclimate community has also tended to take a deterministic view of ice ages, whereas one of the great lessons of weather and climate research has been the role of chaos (Lorenz, 1968). Empirical evidence suggests that changes in orbital parameters, ocean circulation, and atmospheric CO_2, as well as climate memory, are all necessary to explain the spectrum of ice age climate changes (Fig. 7, right)—and no one of these is individually sufficient. Earth System Science was specifically formulated to seek "a scientific understanding of the Earth and its various components, and of the laws that govern its structure and evolution" (National Research Council, 1988). This systems paradigm of climate can accommodate diverse types of forcing, including Milankovitch cycles in orbital insolation forcing, with the variability and complexity of climate emerging from feedbacks among the diverse components of the Earth System (Fig. 7, left).

p0220 Following the best-preserved geologic evidence, much of the effort by the research community has focused on understanding these interactions through the study of the major deglaciations, especially the last deglaciation roughly 18 to 10 thousand years ago. Investigations have led to a prominent explanation for the last deglaciation that exemplifies the multi-dynamic nature of climate change. In this hypothesis, orbital change interacts with millennial-timescale variability to trigger a shutdown in the Atlantic Meridional Overturning Circulation (AMOC). It has been proposed that this shutdown produced boreal cooling and Southern Hemisphere warming, which led to Southern Ocean CO_2 release to the atmosphere, global warming due to the strengthening greenhouse effect, and attendant global deglaciation. This hypothesis has challengers, and it faces apparent discrepancies with some key observations. In particular, ocean circulation models can reproduce the reconstructed AMOC changes of the last deglaciation only when artificially forced with ice sheet meltwater fluxes that are broadly the opposite of the reconstructed ice sheet melt-back history (Snoll et al., 2024). Despite its flaws, the hypothesis illustrates how various combinations of externally determined orbital variation and emergent internal climate system behavior may cause the Earth System to produce ice age cycles with the periodicities of orbital change that are, nevertheless, not completely predictable.

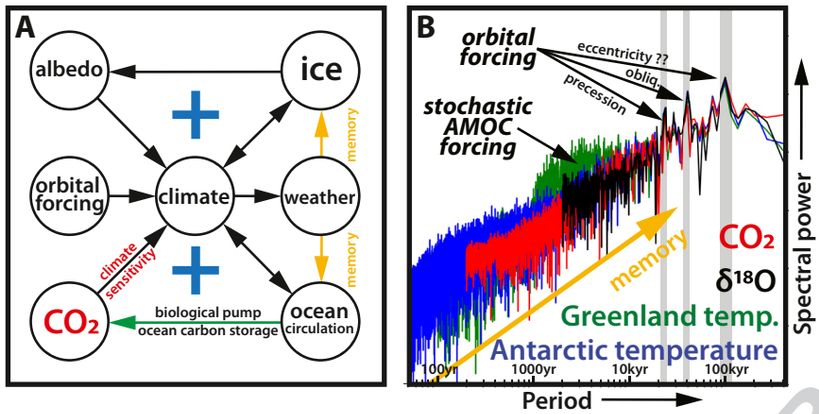

f0040 **Fig. 7** The coupled Earth System dynamics of the late Pleistocene. (A) Changes in albedo, atmospheric CO_2 and orbital forcing cause climate change that can be understood as a change in the statistics of weather, yielding (B) the characteristic spectrum of climate variability. Ocean circulation, the ice sheets, and CO_2 respond to changes in mean climate but also integrate short-term variability. The centennial-scale memory of ocean circulation contributes to millennial-scale variability of Atlantic Meridional Overturning Circulation, while the millennial-timescale memory of the ice sheets contributes to climate variability on orbital timescales. Orbitally-forced changes in ice sheets and global albedo have been found insufficient to explain the magnitude of ice age climate cycles or of their attendant atmospheric CO_2 variations. Changes in biologically-driven deep ocean CO_2 storage (i.e., the biological pump) are thought to explain most of the recorded CO_2 change, thereby significantly contributing to ice age climate change. As such, orbital forcing, the ice–albedo feedback, the ocean–CO_2 feedback and climate system memory are all required elements in explaining the reconstructed spectra of ice age climate change. It remains unclear if stochastic variability on millennial timescales simply detracts from orbital control (determinism) of ice ages cycles, or if the ocean circulation and resulting carbon cycle changes are critical dynamics in the synchronization of ice ages to orbital forcing by obliquity and eccentricity modulation of precession (e.g., by changing the frequency of freshwater discharges to the North Atlantic).

p0225 In comparison to the deglaciations, less attention has been given to the processes developing each of the ice ages in the first place. As described above, there is a degree of consensus that the circulation, biological productivity, and air-sea CO_2 fluxes of the Southern Ocean responded to orbitally paced and/or chaotic internal forcings (e.g., from ice sheets or the ocean) on Southern Hemisphere climate. However, there is fundamental disagreement between climate model simulations and paleoceanographic reconstructions as to the ice age state of the Southern Ocean and by which mechanisms this state induced a lower CO_2 concentration in the atmosphere (Sigman et al., 2021). Reconstructions of a broader range of environmental conditions from before the Mid-Pleistocene Transition, with its different periodicities of ice age cycles, may be needed to identify the Earth System feedbacks that drive ice age development (Hain and Chalk, 2025). In any case, the strong and stable coupling of temperature to atmospheric CO, rather than to orbit, over the late Pleistocene (Siegenthaler et al., 2005) indicates that better understanding of the ice age cycles also advances our understanding of Earth System feedbacks and thereby promotes our capacity to anticipate future changes, both natural and human-caused.

ac0010 Acknowledgments

p9005 M.P.H. gratefully acknowledges sabbatical support from the Harry Hess Visiting Faculty Fund from the Department of Geosciences at Princeton University.

References

Abe-Ouchi A, Saito F, Kawamura K, et al. (2013) Insolation-driven 100,000-year glacial cycles and hysteresis of ice-sheet volume. *Nature* 500(7461): 190–193. https://doi.org/10.1038/nature12374.

Abernathey R and Ferreira D (2015) Southern Ocean isopycnal mixing and ventilation changes driven by winds. *Geophysical Research Letters* 42(23). https://doi.org/10.1002/2015GL066238.

Adhémar JA (1842) *Les Revolutions de la mer*. Carilian-Goeury et Va Dalmont.

Agassiz L (1840) Etudes sur les glaciers. *Jent et Gassmann*. https://lccn.loc.gov/12008544.

Ahn J and Brook EJ (2008) Atmospheric CO_2 and climate on millennial time scales during the last glacial period. *Science* 322(5898): 83–85. https://doi.org/10.1126/science.1160832.

Ai XE, Studer AS, Sigman DM, et al. (2020) Southern ocean upwelling, earth's obliquity, and glacial-interglacial atmospheric CO_2 change. *Science* 370(6522): 1348–1352. https://doi.org/10.1126/science.abd2115.

Alley RB, Clark PU, Huybrechts P, and Joughin I (2005) Ice-sheet and sea-level changes. *Science* 310(5747): 456–460. https://doi.org/10.1126/science.1114613.

Anderson RF, Ali S, Bradtmiller LI, et al. (2009) Wind-driven upwelling in the Southern Ocean and the deglacial rise in atmospheric CO_2. *Science* 323(5920): 1443–1448. https://doi.org/10.1126/science.1167441.

Anderson RF, Sachs JP, Fleisher MQ, et al. (2019) Deep-sea oxygen depletion and ocean carbon sequestration during the last ice age. *Global Biogeochemical Cycles* 33(3): 301–317. https://doi.org/10.1029/2018GB006049.

Archer DE, Martin PA, Milovich J, Brovkin V, Plattner G-K, and Ashendel C (2003) Model sensitivity in the effect of Antarctic sea ice and stratification on atmospheric pCO_2. *Paleoceanography* 18(1): 2002PA000760. https://doi.org/10.1029/2002PA000760.

Archer D, Eby M, Brovkin V, et al. (2009) Atmospheric lifetime of fossil fuel carbon dioxide. *Annual Review of Earth and Planetary Sciences* 37(1): 117–134. https://doi.org/10.1146/annurev.earth.031208.100206.

Arrhenius S (1896) XXXI. On the influence of carbonic acid in the air upon the temperature of the ground. *The London, Edinburgh, and Dublin Philosophical Magazine and Journal of Science* 41(251): 237–276. https://doi.org/10.1080/14786449608620846.

Baker JA, Bell MJ, Jackson LC, Vallis GK, Watson AJ, and Wood RA (2025) Continued Atlantic overturning circulation even under climate extremes. *Nature* 638(8052): 987–994. https://doi.org/10.1038/s41586-024-08544-0.

Barker S, Diz P, Vautravers MJ, et al. (2009) Interhemispheric Atlantic seesaw response during the last deglaciation. *Nature* 457(7233): 1097–1102. https://doi.org/10.1038/nature07770.

Barker S, Gregor Knorr R, Edwards L, et al. (2011) 800,000 years of abrupt climate variability. *Science* 334(6054): 347–351. https://doi.org/10.1126/science.1203580.

Barker S, Starr A, Van Der Lubbe J, et al. (2022) Persistent influence of precession on northern ice sheet variability since the early Pleistocene. *Science* 376(6596): 961–967. https://doi.org/10.1126/science.abm4033.

Barker S, Lisiecki LE, Knorr G, Nuber S, and Tzedakis PC (2025) Distinct roles for precession, obliquity, and eccentricity in Pleistocene 100-Kyr glacial cycles. *Science* 387(6737). https://doi.org/10.1126/science.adp3491. eadp3491.

Barnola JM, Raynaud D, Korotkevich YS, and Lorius C (1987) Vostok ice core provides 160,000-year record of atmospheric CO_2. *Nature* 329(6138): 408–414. https://doi.org/10.1038/329408a0.

Bautsch M and Pedde F (2023) *Canopus Der Stern Der Stadt Eridu"." Mitteilungen, Informationen, Progrm Der Wilhelm-Foerster-Sternwarte e.V Zeiss-Planetarium Am Insulaner.*

Bender M, Sowers T, Dickson M-L, et al. (1994) Climate correlations between Greenland and Antarctica during the Past 100,000 years. *Nature* 372(6507): 663–666. https://doi.org/10.1038/372663a0.

Bereiter B, Eggleston S, Schmitt J, et al. (2015) Revision of the EPICA Dome C CO_2 Record from 800 to 600 Kyr before Present: Analytical Bias in the EDC CO2 Record. *Geophysical Research Letters* 42(2): 542–549. https://doi.org/10.1002/2014GL061957.

Berger WH (1999) The 100-Kyr ice-age cycle: Internal oscillation or inclinational forcing? *International Journal of Earth Sciences* 88(2): 305–316. https://doi.org/10.1007/s005310050266.

Berger WH (2013) On the Milankovitch sensitivity of the quaternary deep-sea record. *Climate of the Past* 9(4): 2003–2011. https://doi.org/10.5194/cp-9-2003-2013.

Berger A (2021) Milankovitch, the father of paleoclimate modeling. *Climate of the Past* 17(4): 1727–1733. https://doi.org/10.5194/cp-17-1727-2021.

Blunier T and Brook EJ (2001) Timing of millennial-scale climate change in Antarctica and Greenland during the last glacial period. *Science* 291(5501): 109–112. https://doi.org/10.1126/science.291.5501.109.

Blunier T, Chappellaz J, Schwander J, et al. (1998) Asynchrony of Antarctic and Greenland climate change during the last glacial period. *Nature* 394(6695): 739–743. https://doi.org/10.1038/29447.

Böhm E, Lippold J, Gutjahr M, et al. (2015) Strong and deep Atlantic meridional overturning circulation during the last glacial cycle. *Nature* 517(7532): 73–76. https://doi.org/10.1038/nature14059.

Bolin B and Stommel H (1961) On the abyssal circulation of the world ocean—IV. *Deep Sea Research (1953)* 8(2): 95–110. https://doi.org/10.1016/0146-6313(61)90002-8.

Boyle EA (1988) The role of vertical chemical fractionation in controlling late quaternary atmospheric carbon dioxide. *Journal of Geophysical Research: Oceans* 93(C12): 15701–15714. https://doi.org/10.1029/JC093iC12p15701.

Broecker WS (1982a) Ocean chemistry during glacial time. *Geochimica et Cosmochimica Acta* 46(10): 1689–1705. https://doi.org/10.1016/0016-7037(82)90110-7.

Broecker WS (1982b) Glacial to interglacial changes in ocean chemistry. *Progress in Oceanography* 11: 151–197.

Broecker WS (1987) The biggest chill. *Natural History Magazine* 97: 74–82.

Broecker WS (1998) Paleocean circulation during the last deglaciation: A bipolar seesaw? *Paleoceanography* 13(2): 119–121. https://doi.org/10.1029/97PA03707.

Broecker WS (2006) Abrupt climate change revisited. *Global and Planetary Change* 54(3–4): 211–215. https://doi.org/10.1016/j.gloplacha.2006.06.019.

Broecker WS and Peng T-H (1987) The role of $CaCO_3$ compensation in the glacial to interglacial atmospheric CO_2 change. *Global Biogeochemical Cycles* 1(1): 15–29. https://doi.org/10.1029/GB001i001p00015.

Broecker WS and Van Donk J (1970) Insolation changes, ice volumes, and the O^{18} record in deep-sea cores. *Reviews of Geophysics* 8(1): 169–198. https://doi.org/10.1029/RG008i001p00169.

Broecker WS, Takahashi T, and Takahashi T (1985) Sources and flow patterns of deep-ocean waters as deduced from potential temperature, salinity, and initial phosphate concentration. *Journal of Geophysical Research* 90(C4): 6925. https://doi.org/10.1029/JC090iC04p06925.

Broeker W (1991) The great ocean conveyor. *Oceanography* 4(2): 79–89. https://doi.org/10.5670/oceanog.1991.07.

Brückner E, Köppen WP, and Wegener A (1925) Über Die Klimate Der Geologischen Vorzeit. *Zeitschrift Für Gletscherkunde (Berlin)* 14: 149–169.

Bryan F (1987) Parameter sensitivity of primitive equation ocean general circulation models. *Journal of Physical Oceanography* 17(7): 970–985. https://doi.org/10.1175/1520-0485(1987)017%253C0970:PSOPEO%253E2.0.CO;2.

Budyko MI (1969) The effect of solar radiation variations on the climate of the Earth. *Tellus* 21(5): 611–619. https://doi.org/10.1111/j.2153-3490.1969.tb00466.x.

Callendar GS (1938) The artificial production of carbon dioxide and its influence on temperature: The artificial production of carbon dioxide. *Quarterly Journal of the Royal Meteorological Society* 64(275): 223–240. https://doi.org/10.1002/qj.49706427503.

Callendar GS (1949) Can carbon dioxide influence climate? *Weather* 4(10): 310–314. https://doi.org/10.1002/j.1477-8696.1949.tb00952.x.

Calov R and Ganopolski A (2005) Multistability and hysteresis in the climate-cryosphere system under orbital forcing. *Geophysical Research Letters* 32(21). https://doi.org/10.1029/2005GL024518. 2005GL024518.

Capron E, Landais A, Lemieux-Dudon B, et al. (2010) Synchronising EDML and NorthGRIP ice cores using δ18O of atmospheric oxygen (δ18Oatm) and CH4 measurements over MIS5 (80–123 Kyr). *Quaternary Science Reviews* 29(1–2): 222–234. https://doi.org/10.1016/j.quascirev.2009.07.014.

Capron E, Govin A, Stone EJ, et al. (2014) Temporal and spatial structure of multi-millennial temperature changes at high latitudes during the last interglacial. *Quaternary Science Reviews* 103: 116–133. https://doi.org/10.1016/j.quascirev.2014.08.018.

Chalk TB, Hain MP, Foster GL, et al. (2017) Causes of ice age intensification across the mid-Pleistocene transition. *Proceedings of the National Academy of Sciences* 114(50): 13114–13119. https://doi.org/10.1073/pnas.1702143114.

Chamberlin TC (1894) Glacial phenomena of North America. In: Geike J (ed.) *The Great Ice Age: And Its Relation to the Antiquity of Man*, 3rd edn. D. Appleton and Company. https://books.google.com/books?id=SEfttJ-_iMoC&pg=PA724&source=gbs_toc_r&cad=2.

Chamberlin TC (1897) A group of hypotheses bearing on climatic changes. *The Journal of Geology (Chicago)* 5(7): 653–683.

Chamberlin TC (1899) An attempt to frame a working hypothesis of the cause of glacial periods on an atmospheric basis. *The Journal of Geology* 7(6): 545–584. https://doi.org/10.1086/608449.

Chang L, Hoogakker BAA, Heslop D, et al. (2023) Indian Ocean glacial deoxygenation and respired carbon accumulation during mid-late quaternary ice ages. *Nature Communications* 14(1): 4841. https://doi.org/10.1038/s41467-023-40452-1.

Charney JG, et al. (1979) Ad hoc study group on carbon dioxide and climate, climate research board, assembly of mathematical and physical sciences, and national research council. In: *Carbon Dioxide and Climate: A Scientific Assessment*. National Academies Press. https://doi.org/10.17226/12181.

Chen Z, Hobbs W, Chase Z, and Zika J (2025) The impact of Antarctic Sea Ice on Southern Ocean water mass transformation in coupled climate models. *Journal of Geophysical Research: Oceans* 130(9). https://doi.org/10.1029/2025JC022445. e2025JC022445.

Cheng H, Lawrence Edwards R, Broecker WS, et al. (2009) Ice age terminations. *Science* 326(5950): 248–252. https://doi.org/10.1126/science.1177840.

Chiang JCH and Broccoli AJ (2024) Orbital eccentricity and Earth's seasonal cycle. *PLOS Climate* 3(7): e0000436. https://doi.org/10.1371/journal.pclm.0000436.

Chiang JCH and Koutavas A (2004) Tropical flip-flop connections. *Nature* 432(7018): 684–685. https://doi.org/10.1038/432684a.

Clark PU and Pollard D (1998) Origin of the Middle Pleistocene Transition by ice sheet erosion of regolith. *Paleoceanography* 13(1): 1–9. https://doi.org/10.1029/97PA02660.

Clark PU, Shakun JD, Baker PA, et al. (2012) Global climate evolution during the last deglaciation. *Proceedings of the National Academy of Sciences* 109(19). https://doi.org/10.1073/pnas.1116619109.

CLIMAP Project Members (1976) The surface of the ice-age Earth: Quantitative geologic evidence is used to reconstruct boundary conditions for the climate 18,000 years ago. *Science* 191(4232): 1131–1137. https://doi.org/10.1126/science.191.4232.1131.

Crichton KA, Bouttes N, Roche DM, Chappellaz J, and Krinner G (2016) Permafrost carbon as a missing link to explain CO_2 changes during the last deglaciation. *Nature Geoscience* 9(9): 683–686. https://doi.org/10.1038/ngeo2793.

Croll J (1864) XIII. On the physical cause of the change of climate during geological epochs. *The London, Edinburgh, and Dublin Philosophical Magazine and Journal of Science* 28(187): 121–137. https://doi.org/10.1080/14786446408643733.

Croll J (1867) XVII. On the excentricity of the Earth's orbit, and its physical relations to the glacial epoch. *The London, Edinburgh, and Dublin Philosophical Magazine and Journal of Science* 33(221): 119–131. https://doi.org/10.1080/14786446708639757.

Croll J (1875) *Climate and Time, in Their Geological Relations, a Theory of Secular Changes of the Earth's Climate*. Edward Stanford.

Crucifix M (2013) Why could ice ages be unpredictable? *Climate of the Past* 9(5): 2253–2267. https://doi.org/10.5194/cp-9-2253-2013.

Curry WB and Oppo DW (2005) Glacial water mass geometry and the distribution of $\delta^{13}C$ of ΣCO_2 in the Western Atlantic Ocean: Glacial water mass geometry. *Paleoceanography* 20(1). https://doi.org/10.1029/2004PA001021.

Dansgaard W, Clausen HB, Gundestrup N, et al. (1982) A new Greenland deep ice core. *Science* 218(4579): 1273–1277. https://doi.org/10.1126/science.218.4579.1273.

Dansgaard W, Johnsen SJ, Clausen HB, et al. (1984) North Atlantic climatic oscillations revealed by deep Greenland Ice Cores. In: Hansen JE and Takahashi T (eds.) *Geophysical Monograph Series*, 29. American Geophysical Union. https://doi.org/10.1029/GM029p0288.

Dansgaard W, Johnsen SJ, Clausen HB, et al. (1993) Evidence for general instability of past climate from a 250-Kyr ice-core record. *Nature* 364(6434): 218–220. https://doi.org/10.1038/364218a0.

Delmas RJ, Ascencio J-M, and Legrand M (1980) Polar ice evidence that atmospheric CO_2 20,000 Yr BP was 50% of present. *Nature* 284(5752): 155–157. https://doi.org/10.1038/284155a0.

Denton GH, Anderson RF, Toggweiler JR, Edwards RL, Schaefer JM, and Putnam AE (2010) The last glacial termination. *Science* 328(5986): 1652–1656. https://doi.org/10.1126/science.1184119.

Deschamps P, Durand N, Bard E, et al. (2012) Ice-sheet collapse and sea-level rise at the bølling warming 14,600 years ago. *Nature* 483(7391): 559–564. https://doi.org/10.1038/nature10902.

DeVries T and Primeau F (2011) Dynamically and observationally constrained estimates of water-mass distributions and ages in the global ocean. *Journal of Physical Oceanography* 41(12): 2381–2401. https://doi.org/10.1175/JPO-D-10-05011.1.

Ditlevsen P and Ditlevsen S (2023) Warning of a forthcoming collapse of the Atlantic meridional overturning circulation. *Nature Communications* 14(1): 4254. https://doi.org/10.1038/s41467-023-39810-w.

Donohoe A, Fajber R, Cox T, Armour KC, Battisti DS, and Roe GH (2024) Model biases in the atmosphere-ocean partitioning of poleward heat transport are persistent across three CMIP generations. *Geophysical Research Letters* 51(8): e2023GL106639. https://doi.org/10.1029/2023GL106639.

Drijfhout S, Angevaare JR, Mecking J, Van Westen RM, and Rahmstorf S (2025) Shutdown of northern Atlantic overturning after 2100 following deep mixing collapse in CMIP6 projections. *Environmental Research Letters* 20(9): 094062. https://doi.org/10.1088/1748-9326/adfa3b.

Duplessy JC, Shackleton NJ, Fairbanks RG, Labeyrie L, Oppo D, and Kallel N (1988) Deepwater source variations during the last climatic cycle and their impact on the global deepwater circulation. *Paleoceanography* 3(3): 343–360. https://doi.org/10.1029/PA003i003p00343.

Esmark J (1824) Bidrag Til Vor Jorklodes Historie. *Nyt Magazin for Naturvidenskaberne*: 28–49.

Etminan M, Myhre G, Highwood EJ, and Shine KP (2016) Radiative forcing of carbon dioxide, methane, and nitrous oxide: A significant revision of the methane radiative forcing. *Geophysical Research Letters* 43(24). https://doi.org/10.1002/2016GL071930.

Faegre A (1972) An intransitive model of the earth-atmosphere-ocean system. *Journal of Applied Meteorology* 11(1): 4–6. https://doi.org/10.1175/1520-0450(1972)011%253C0004:AIMOTE%253E2.0.CO;2.

Ferrari R, Jansen MF, Adkins JF, Burke A, Stewart AL, and Thompson AF (2014) Antarctic sea ice control on ocean circulation in present and glacial climates. *Proceedings of the National Academy of Sciences* 111(24): 8753–8758. https://doi.org/10.1073/pnas.1323922111.

Fleming JR (1998) *Historical Perspectives on Climate Change*. Oxford Scholarship Online, Oxford University Press. https://doi.org/10.1093/oso/9780195078701.001.0001.

Foote E (1856) Circumstances affecting the heat of sun's rays. *American Journal of Art and Science* 22(66): 382–383. https://publicdomainreview.org/collection/first-paper-to-link-co2-and-global-warming-by-eunice-foote-1856/.

Fourier J-B-J (1822) *Theorie Analytique de La Chaleur*. Cambridge University Press. http://ebooks.cambridge.org/ebook.jsf?bid=CBO9780511693229.

Fox-Kemper B, Hewitt HT, Xiao C, Aðalgeirsdóttir G, Drijfhout SS, Edwards TL, Golledge NR, Hemer M, Kopp RE, Krinner G, Mix A, Notz D, Nowicki S, Nurhati IS, Ruiz L, Sallée J-B, and Slangen ABA (2021) Ocean, cryosphere and sea level change. In: Masson-Delmotte V, Zhai P, Pirani A, Connors SL, Péan C, Berger S, Caud N, Chen Y, Goldfarb L, Gomis MI, Huang M, Leitzell K, Lonnoy E, Matthews JBR, Maycock TK, Waterfield T, Yelekçi O, Yu R, and Zhou B (eds.) *Climate Change 2021: The Physical Science Basis. Contribution of Working Group I to the Sixth Assessment Report of the Intergovernmental Panel on Climate Change*, pp. 1211–1362. Cambridge, United Kingdom and New York, NY: Cambridge University Press. https://doi.org/10.1017/9781009157896.011.

François R, Altabet MA, Ein-Fen Y, et al. (1997) Contribution of southern ocean surface-water stratification to low atmospheric CO_2 concentrations during the last glacial period. *Nature* 389(6654): 929–935. https://doi.org/10.1038/40073.

Frankignoul C and Hasselmann K (1977) Stochastic climate models, part ii application to sea-surface temperature anomalies and thermocline variability. *Tellus* 29(4): 289–305. https://doi.org/10.1111/j.2153-3490.1977.tb00740.x.

Galbraith E and De Lavergne C (2019) Response of a comprehensive climate model to a broad range of external forcings: Relevance for deep ocean ventilation and the development of late cenozoic ice ages. *Climate Dynamics* 52(1–2): 653–679. https://doi.org/10.1007/s00382-018-4157-8.

Ganopolski A (2024) Toward generalized Milankovitch theory (GMT). *Climate of the Past* 20(1): 151–185. https://doi.org/10.5194/cp-20-151-2024.

Ganopolski A, Calov R, and Claussen M (2010) Simulation of the last glacial cycle with a coupled climate ice-sheet model of intermediate complexity. *Climate of the Past* 6(2): 229–244. https://doi.org/10.5194/cp-6-229-2010.

Garbe J, Albrecht T, Levermann A, Donges JF, and Winkelmann R (2020) The hysteresis of the Antarctic ice sheet. *Nature* 585(7826): 538–544. https://doi.org/10.1038/s41586-020-2727-5.

Gardner AS and Sharp MJ (2010) A review of snow and ice albedo and the development of a new physically based broadband albedo parameterization. *Journal of Geophysical Research: Earth Surface* 115(F1). https://doi.org/10.1029/2009JF001444. 2009JF001444.

Gebbie G and Huybers P (2010) Total matrix intercomparison: A method for determining the geometry of water-mass pathways. *Journal of Physical Oceanography* 40(8): 1710–1728. https://doi.org/10.1175/2010JPO4272.1.

Geike J (1894) *The Great Ice Age: And Its Relation to the Antiquity of Man*, 3rd edn. D. Appleton and Company.

Genthon G, Barnola JM, Raynaud D, et al. (1987) Vostok ice core: Climatic response to CO_2 and orbital forcing changes over the last climatic cycle. *Nature* 329(6138): 414–418. https://doi.org/10.1038/329414a0.

Ghil M and Lucarini V (2020) The physics of climate variability and climate change. *Reviews of Modern Physics* 92(3): 035002. https://doi.org/10.1103/RevModPhys.92.035002.

Ghil M, Allen MR, Dettinger MD, et al. (2002) Advanced spectral methods for climatic time series. *Reviews of Geophysics* 40(1). https://doi.org/10.1029/2000RG000092.

Gray WR, Rae JWB, Wills RCJ, et al. (2018) Deglacial upwelling, productivity and CO_2 outgassing in the North Pacific Ocean. *Nature Geoscience* 11(5): 340–344. https://doi.org/10.1038/s41561-018-0108-6.

Gregoire LJ, Payne AJ, and Valdes PJ (2012) Deglacial rapid sea level rises caused by ice-sheet saddle collapses. *Nature* 487(7406): 219–222. https://doi.org/10.1038/nature11257.

Greve R and Blatter H (2009) *Dynamics of Ice Sheets and Glaciers. Advances in Geophysical and Environmental Mechanics and Mathematics*. Springer.

Gutiérrez-González L, Robinson A, Alvarez-Solas J, et al. (2025) *Hysteresis of the Greenland Ice Sheet from the Last Glacial Maximum to the Future*. Preprint, Ice sheets/Greenland, July 15, 2025, https://doi.org/10.5194/egusphere-2025-2616.

Hain MP and Sigman DM (2024) CO2 in Earth's Ice Age cycles. In: *Oxford Research Encyclopedia of Climate Science*, by Hain MP and Sigman DM. Oxford University Press. doi:https://doi.org/10.1093/acrefore/9780190228620.013.879.

Hain MP and Chalk TB (2025) Greenhouse gas effects on quaternary climates. In: *Reference Module in Earth Systems and Environmental Sciences*. Elsevier. https://doi.org/10.1016/B978-0-323-99931-1.00271-3.

Hain MP, Sigman DM, and Haug GH (2010) Carbon dioxide effects of Antarctic stratification, North Atlantic intermediate water formation, and subantarctic nutrient drawdown during the last ice age: Diagnosis and synthesis in a geochemical box model: Atmospheric CO_2 during the last ice age. *Global Biogeochemical Cycles* 24(4). https://doi.org/10.1029/2010GB003790.

Hain MP, Sigman DM, and Haug GH (2014) The biological pump in the past. In: *Treatise on Geochemistry*. Elsevier. https://doi.org/10.1016/B978-0-08-095975-7.00618-5.

Hall BL, Putnam AE, Lowell TV, et al. (2026) Rapid thinning of the cordillera darwin icefield at the onset of termination I. *Quaternary Science Reviews* 373: 109754. https://doi.org/10.1016/j.quascirev.2025.109754.

Hasselmann K (1976) Stochastic climate models part I. Theory. *Tellus* 28(6): 473–485. https://doi.org/10.1111/j.2153-3490.1976.tb00696.x.

Haug GH, Tiedemann R, Zahn R, and Christina Ravelo A (2001) Role of Panama uplift on oceanic freshwater balance. *Geology* 29(3). https://doi.org/10.1130/0091-7613(2001)029%253C0207:ROPUOO%253E2.0.CO;2.

Hays JD, Imbrie J, and Shackleton NJ (1976) Variations in the Earth's orbit: Pacemaker of the ice ages: For 500,000 years, major climatic changes have followed variations in obliquity and precession. *Science* 194(4270): 1121–1132. https://doi.org/10.1126/science.194.4270.1121.

Heinrich H (1988) Origin and consequences of cyclic ice rafting in the Northeast Atlantic Ocean during the past 130,000 years. *Quaternary Research* 29(2): 142–152. https://doi.org/10.1016/0033-5894(88)90057-9.

Herschel JFW (1832) XVII.—On the astronomical causes which may influence geological phænomena. *Transactions of the Geological Society of London* 3(2): 293–300. https://doi.org/10.1144/transgslb.3.2.293.

Hines SKV, Foukal NP, Costa KM, Oppo DW, Marchal O, Keigwin LD, and Condron A (2025) Is there robust evidence for freshwater-driven AMOC changes? A synthesis of data, models, and mechanisms. *Oceanography* 38(3): 12–23. https://doi.org/10.5670/oceanog.2025.e301.

Hobart B, Lisiecki LE, Rand D, Lee T, and Lawrence CE (2023) Late Pleistocene 100-Kyr glacial cycles paced by precession forcing of summer insolation. *Nature Geoscience* 16(8): 717–722. https://doi.org/10.1038/s41561-023-01235-x.

Hodell DA, Channell JET, Curtis JH, Romero OE, and Röhl U (2008) Onset of 'Hudson Strait' Heinrich events in the Eastern North Atlantic at the end of the middle Pleistocene transition (~640 Ka)? *Paleoceanography* 23(4). https://doi.org/10.1029/2008PA001591. 2008PA001591.

Hodell DA, Nicholl JA, Bontognali TRR, et al. (2017) Anatomy of Heinrich layer 1 and its role in the last deglaciation: Heinrich event 1. *Paleoceanography* 32(3): 284–303. https://doi.org/10.1002/2016PA003028.

Hoffman PF, Kaufman AJ, Halverson GP, and Schrag DP (1998) A neoproterozoic snowball Earth. *Science* 281(5381): 1342–1346. https://doi.org/10.1126/science.281.5381.1342.

Hoogakker BAA, Zunli L, Umling N, et al. (2018) Glacial expansion of oxygen-depleted seawater in the Eastern Tropical Pacific. *Nature* 562(7727): 410–413. https://doi.org/10.1038/s41586-018-0589-x.

Huybers P (2006) Early Pleistocene glacial cycles and the integrated summer insolation forcing. *Science* 313(5786): 508–511. https://doi.org/10.1126/science.1125249.

Huybers P (2011) Combined obliquity and precession pacing of late Pleistocene deglaciations. *Nature* 480(7376): 229–232. https://doi.org/10.1038/nature10626.

Huybers P and Curry W (2006) Links between annual, Milankovitch and continuum temperature variability. *Nature* 441(7091): 329–332. https://doi.org/10.1038/nature04745.

Huybers P and Tziperman E (2008) Integrated summer insolation forcing and 40,000-year glacial cycles: The perspective from an ice-sheet/energy-balance model. *Paleoceanography* 23(1). https://doi.org/10.1029/2007PA001463. 2007PA001463.

Huybers P and Wunsch C (2005) Obliquity pacing of the late Pleistocene glacial terminations. *Nature* 434(7032): 491–494. https://doi.org/10.1038/nature03401.

Imbrie J and Imbrie JZ (1980) Modeling the climatic response to orbital variations. *Science* 207(4434): 943–953. https://doi.org/10.1126/science.207.4434.943.

Imbrie J and Imbrie KP (1986) *Ice Ages: Solving the Mystery*. Harvard University Press, ISBN: 978-0-674-44075-3.

Imbrie J, Hayes JD, Douglas GM, and McIntyre A (1984) The orbital theory of Pleistocene climate: Support from a revised chronology of the marine δ18o record. In: *Milankovitch and Climate, Part 1*. D. Reidel Publishing Co.

Imbrie J, Boyle EA, Clemens SC, et al. (1992) On the structure and origin of major glaciation cycles 1. Linear responses to Milankovitch forcing. *Paleoceanography* 7(6): 701–738. https://doi.org/10.1029/92PA02253.

Imbrie J, Berger A, Boyle EA, et al. (1993) On the structure and origin of major glaciation cycles 2. The 100,000-year cycle. *Paleoceanography* 8(6): 699–735. https://doi.org/10.1029/93PA02751.

Jaccard SL, Hayes CT, Martínez-García A, et al. (2013) Two modes of change in southern ocean productivity over the past million years. *Science* 339(6126): 1419–1423. https://doi.org/10.1126/science.1227545.

Jacobel AW, Anderson RF, Jaccard SL, McManus JF, Pavia FJ, and Winckler G (2020) Deep pacific storage of respired carbon during the last ice age: Perspectives from bottom water oxygen reconstructions. *Quaternary Science Reviews* 230: 106065. https://doi.org/10.1016/j.quascirev.2019.106065.

Jansen MF (2017) Glacial ocean circulation and stratification explained by reduced atmospheric temperature. *Proceedings of the National Academy of Sciences* 114(1): 45–50. https://doi.org/10.1073/pnas.1610438113.

Jeltsch-Thömmes A, Battaglia G, Cartapanis O, Jaccard SL, and Joos F (2019) Low terrestrial carbon storage at the last glacial maximum: Constraints from multi-proxy data. *Climate of the Past* 15(2): 849–879. https://doi.org/10.5194/cp-15-849-2019.

Jiao N, Herndl GJ, Hansell DA, et al. (2010) Microbial production of recalcitrant dissolved organic matter: Long-term carbon storage in the global ocean. *Nature Reviews Microbiology* 8(8): 593–599. https://doi.org/10.1038/nrmicro2386.

Johnsen SJ, Clausen HB, Dansgaard W, et al. (1992) Irregular glacial interstadials recorded in a new Greenland ice core. *Nature* 359(6393): 311–313. https://doi.org/10.1038/359311a0.

Jouzel J, Masson-Delmotte V, Cattani O, et al. (2007) Orbital and millennial Antarctic climate variability over the past 800,000 years. *Science* 317(5839): 793–796. https://doi.org/10.1126/science.1141038.

Kawamura K, Parrenin F, Lisiecki L, et al. (2007) Northern hemisphere forcing of climatic cycles in Antarctica over the past 360,000 years. *Nature* 448(7156): 912–916. https://doi.org/10.1038/nature06015.

Khatiwala S, Schmittner A, and Muglia J (2019) Air-sea disequilibrium enhances ocean carbon storage during glacial periods. *Science Advances* 5(6). https://doi.org/10.1126/sciadv.aaw4981. eaaw4981.

Killworth PD (1983) Deep convection in the World Ocean. *Reviews of Geophysics* 21(1): 1–26. https://doi.org/10.1029/RG021i001p00001.
Kirschvink JL (1992) Late proterozoic low-latitude global glaciation: The snowball Earth. In: *The Proterozoic Biosphere: A Multidisciplinary Study*. Cambridge University Press.
Knox F and McElroy MB (1984) Changes in atmospheric CO_2: Influence of the marine biota at high latitude. *Journal of Geophysical Research* 89(D3): 4629. https://doi.org/10.1029/JD089iD03p04629.
Koepnick K and Tziperman E (2024) Distinguishing between insolation-driven and phase-locked 100-Kyr ice age scenarios using example models. *Paleoceanography and Paleoclimatology* 39(3): e2023PA004739. https://doi.org/10.1029/2023PA004739.
Köhler P and Van De Wal RSW (2020) Interglacials of the Quaternary defined by northern hemispheric land ice distribution outside of Greenland. *Nature Communications* 11(1): 5124. https://doi.org/10.1038/s41467-020-18897-5.
Köhler P, Bintanja R, Fischer H, et al. (2010) What caused Earth's temperature variations during the last 800,000 years? Data-based evidence on radiative forcing and constraints on climate sensitivity. *Quaternary Science Reviews* 29(1–2): 129–145. https://doi.org/10.1016/j.quascirev.2009.09.026.
Krüger T (2013) Discovering the ice ages: International reception and consequences for a historical understanding of climate. In: *History of Science and Medicine Library*, vol. 37. Brill.
Kuhlbrodt T, Griesel A, Montoya M, Levermann A, Hofmann M, and Rahmstorf S (2007) On the driving processes of the Atlantic meridional overturning circulation. *Reviews of Geophysics* 45(2). https://doi.org/10.1029/2004RG000166. 2004RG000166.
Kumar N, Anderson RF, Mortlock RA, et al. (1995) Increased biological productivity and export production in the glacial southern ocean. *Nature* 378(6558): 675–680. https://doi.org/10.1038/378675a0.
Kwon EY, Hain MP, Sigman DM, Galbraith ED, Sarmiento JL, and Toggweiler JR (2012) North Atlantic ventilation of 'Southern-sourced' deep water in the glacial ocean. *Paleoceanography* 27(2). https://doi.org/10.1029/2011PA002211. 2011PA002211.
Landais A, Masson-Delmotte V, Capron E, et al. (2016) How Warm Was Greenland during the Last Interglacial Period? *Climate of the Past* 12(9): 1933–1948. https://doi.org/10.5194/cp-12-1933-2016.
Langley SP (1890) III. *The Temperature of the Moon. From Studies at the Allegheny Observatory by* S. P. Langley, *with the Assistance of* F. W. Very. *The London, Edinburgh, and Dublin Philosophical Magazine and Journal of Science* 29(176): 31–54. https://doi.org/10.1080/14786449008619903.
Le Verrier U-J (1846) *Recherches Sur Les Mouvements de La Planète Herschel*, 1st edn. Imprimeur-Libraire: Bachelier.
Leduc G, Schneider R, Kim J-H, and Lohmann G (2010) Holocene and eemian sea surface temperature trends as revealed by alkenone and Mg/Ca paleothermometry. *Quaternary Science Reviews* 29(7–8): 989–1004. https://doi.org/10.1016/j.quascirev.2010.01.004.
Leloup G, Quiquet A, Roche DM, Dumas C, and Paillard D (2025) Hysteresis of the Antarctic ice sheet with a coupled climate-ice-sheet model. *Geophysical Research Letters* 52(5). https://doi.org/10.1029/2024GL111492. e2024GL111492.
Levermann A and Winkelmann R (2016) A simple equation for the melt elevation feedback of ice sheets. *The Cryosphere* 10(4): 1799–1807. https://doi.org/10.5194/tc-10-1799-2016.
Lindgren A, Hugelius G, and Kuhry P (2018) Extensive loss of past permafrost carbon but a net accumulation into present-day soils. *Nature* 560(7717): 219–222. https://doi.org/10.1038/s41586-018-0371-0.
Lisiecki LE (2010) Links between eccentricity forcing and the 100,000-year glacial cycle. *Nature Geoscience* 3(5): 349–352. https://doi.org/10.1038/ngeo828.
Lisiecki LE and Raymo ME (2005) A Pliocene-pleistocene stack of 57 globally distributed benthic $\delta^{18}O$ records: Pliocene-Pleistocene benthic stack. *Paleoceanography* 20(1). https://doi.org/10.1029/2004PA001071.
Liu H, Liu Y, Lorraine Lisiecki Y, Gao MZ, and Lin Q (2025) Collapse of the Atlantic meridional ocean circulation induced by precession: Sensitivity to orbital acceleration. *Geophysical Research Letters* 52, no. 18. https://doi.org/10.1029/2025GL115941. e2025GL115941.
Lorenz EN (1955) Available potential energy and the maintenance of the general circulation. *Tellus* 7(2): 157–167. https://doi.org/10.1111/j.2153-3490.1955.tb01148.x.
Lorenz EN (1963) Deterministic nonperiodic flow. *Journal of the Atmospheric Sciences* 20(2): 130–141. https://doi.org/10.1175/1520-0469(1963)020%253C0130:DNF%253E2.0.CO;2.
Lorenz EN (1964) The problem of deducing the climate from the governing equations. *Tellus* 16(1): 1–11. https://doi.org/10.1111/j.2153-3490.1964.tb00136.x.
Lorenz EN (1968) Climate determinism. *Meteorological Monographs* 25: 1–3.
Lüthi D, Le Floch M, Bereiter B, et al. (2008) High-resolution carbon dioxide concentration record 650,000–800,000 years before present. *Nature* 453(7193): 379–382. https://doi.org/10.1038/nature06949.
Lynch-Stieglitz J, Adkins JF, Curry WB, et al. (2007) Atlantic meridional overturning circulation during the last glacial maximum. *Science* 316(5821): 66–69. https://doi.org/10.1126/science.1137127.
Macdonald FA, Schmitz MD, Crowley JL, et al. (2010) Calibrating the cryogenian. *Science* 327(5970): 1241–1243. https://doi.org/10.1126/science.1183325.
Manabe S and Bryan K (1985) CO_2-induced change in a coupled ocean-atmosphere model and its paleoclimatic implications. *Journal of Geophysical Research: Oceans* 90(C6): 11689–11707. https://doi.org/10.1029/JC090iC06p11689.
Manabe S and Stouffer RJ (1988) Two stable equilibria of a coupled ocean-atmosphere model. *Journal of Climate* 1(9): 841–866.
Manabe S and Stouffer RJ (1999) Are two modes of thermohaline circulation stable? *Tellus A: Dynamic Meteorology and Oceanography* 51(3): 400. https://doi.org/10.3402/tellusa.v51i3.13461.
Manabe S and Wetherald RT (1975) The effects of doubling the CO_2 concentration on the climate of a general circulation model. *Journal of the Atmospheric Sciences* 32(1): 3–15. https://doi.org/10.1175/1520-0469(1975)032%253C0003:TEODTC%253E2.0.CO;2.
Marcott SA, Bauska TK, Buizert C, et al. (2014) Centennial-scale changes in the global carbon cycle during the last deglaciation. *Nature* 514(7524): 616–619. https://doi.org/10.1038/nature13799.
Martínez-García A, Sigman DM, Ren H, et al. (2014) Iron fertilization of the Subantarctic Ocean during the last ice age. *Science* 343(6177): 1347–1350. https://doi.org/10.1126/science.1246848.
Marzocchi A and Jansen MF (2019) Global cooling linked to increased glacial carbon storage via changes in Antarctic sea ice. *Nature Geoscience* 12(12): 1001–1005. https://doi.org/10.1038/s41561-019-0466-8.
Maslin MA and Ridgwell AJ (2005) Mid-Pleistocene revolution and the 'Eccentricity Myth.'. *Geological Society, London, Special Publications* 247(1): 19–34. https://doi.org/10.1144/GSL.SP.2005.247.01.02.
McManus JF, Francois R, Gherardi J-M, Keigwin LD, and Brown-Leger S (2004) Collapse and rapid resumption of Atlantic meridional circulation linked to deglacial climate changes. *Nature* 428(6985): 834–837. https://doi.org/10.1038/nature02494.
Milankovitch M (1920) *Théorie Mathématique Des Phénomènes Thermiques Produits Par La Radiation Solaire*. Gauthiers-Villars.
Milankovitch M (1930) Mathematische Klimalehre Und Astronomische Theorie Der Klimaschwankungen. In: *Allgemeine Klimalehre*, 1. Handbuch Der Klimatologie. Borntraeger.
Milankovitch M (1941) *Kanon Der Erdbestrahlung Und Seine Anwendung Auf Das Eiszeitenproblem*, 132. Belgrade: Royal Serbian Academy Special Publications.
Mitsui T, Ditlevsen P, Boers N, and Crucifix M (2025) 100 Kyr Ice age cycles as a timescale-matching problem. *Earth System Dynamics* 16(5): 1569–1584. https://doi.org/10.5194/esd-16-1569-2025.
Monnin E, Indermühle A, Dällenbach A, et al. (2001) Atmospheric CO_2 concentrations over the last glacial termination. *Science* 291(5501): 112–114. https://doi.org/10.1126/science.291.5501.112.
Monselesan DP, O'Kane TJ, Risbey JS, and Church J (2015) Internal climate memory in observations and models. *Geophysical Research Letters* 42(4): 1232–1242. https://doi.org/10.1002/2014GL062765.
Morland LW, Smith GD, and Boulton GS (1984) Basal sliding relations deduced from Ice-sheet data. *Journal of Glaciology* 30(105): 131–139. https://doi.org/10.3189/S0022143000005864.

Muller RA and MacDonald GJ (1997) Glacial cycles and astronomical forcing. *Science* 277(5323): 215–218. https://doi.org/10.1126/science.277.5323.215.
Munk WH (1950) On the wind-driven ocean circulation. *Journal of Meteorology* 7(2): 80–93. https://doi.org/10.1175/1520-0469(1950)007%253C0080:OTWDOC%253E2.0.CO;2.
Munk WH (1966) Abyssal recipes. *Deep Sea Research and Oceanographic Abstracts* 13(4): 707–730. https://doi.org/10.1016/0011-7471(66)90602-4.
National Research Council. (1988) *Earth System Science: A Closer View*. National Academies Press. https://doi.org/10.17226/19088.
Naughton F, Sánchez-Goñi MF, Landais A, Rodrigues T, Riveiros NV, and Toucanne S (2023) The Bølling–Allerød Interstadial. In: *European Glacial Landscapes*. Elsevier. https://doi.org/10.1016/B978-0-323-91899-2.00015-2.
NEEM community members (2013) Eemian Interglacial Reconstructed from a Greenland Folded Ice Core. *Nature* 493(7433): 489–494. https://doi.org/10.1038/nature11789.
Neftel A, Oeschger H, Schwander J, Stauffer B, and Zumbrunn R (1982) Ice core sample measurements give atmospheric CO_2 content during the past 40,000 Yr. *Nature* 295(5846): 220–223. https://doi.org/10.1038/295220a0.
Niu L, Knorr G, Krebs-Kanzow U, Gierz P, and Lohmann G (2024) Rapid Laurentide Ice Sheet growth preceding the Last Glacial Maximum due to summer snowfall. *Nature Geoscience* 17(5): 440–449. https://doi.org/10.1038/s41561-024-01419-z.
North Greenland Ice Core Project members (2004) High-resolution record of northern hemisphere climate extending into the last interglacial period. *Nature* 431(7005): 147–151. https://doi.org/10.1038/nature02805.
Orsi AH, Smethie WM, and Bullister JL (2002) On the total input of Antarctic waters to the Deep Ocean: A preliminary estimate from chlorofluorocarbon measurements. *Journal of Geophysical Research: Oceans* 107(C8). https://doi.org/10.1029/2001JC000976.
Otto-Bliesner BL, Hewitt CD, Marchitto TM, et al. (2007) Last glacial maximum ocean thermohaline circulation: PMIP2 model intercomparisons and data constraints. *Geophysical Research Letters* 34(12). https://doi.org/10.1029/2007GL029475. 2007GL029475.
Paillard D (1998) The timing of Pleistocene glaciations from a simple multiple-state climate model. *Nature* 391(6665): 378–381. https://doi.org/10.1038/34891.
Paillard D (2001) Glacial cycles: Toward a new paradigm. *Reviews of Geophysics* 39(3): 325–346. https://doi.org/10.1029/2000RG000091.
Parrenin F and Paillard D (2012) Terminations VI and VIII (∼ 530 and ∼ 720 Kyr BP) tell us the importance of obliquity and precession in the triggering of deglaciations. *Climate of the Past* 8(6): 2031–2037. https://doi.org/10.5194/cp-8-2031-2012.
Peltier WR (2005) On the hemispheric origins of meltwater pulse 1a. *Quaternary Science Reviews* 24(14–15): 1655–1671. https://doi.org/10.1016/j.quascirev.2004.06.023.
Penck A (1879) *Die Geschiebeformation Norddeutschlands*. Zeitschrift Der Deutschen Geologische Gesellschaft.
Penck A (1938) Die Strahlungstheorie Und Die Geologische Zeitrechnung. *Zeitschrift Der Gesellschaft Für Erdkunde Zu Berlin* (9/10): 321–350.
Peterson LC, Haug GH, Hughen KA, and Röhl U (2000) Rapid changes in the hydrologic cycle of the tropical Atlantic during the last glacial. *Science* 290(5498): 1947–1951. https://doi.org/10.1126/science.290.5498.1947.
Peterson CD, Lisiecki LE, and Stern JV (2014) Deglacial whole-ocean $\delta^{13}C$ change estimated from 480 benthic foraminiferal records. *Paleoceanography* 29(6): 549–563. https://doi.org/10.1002/2013PA002552.
Petit JR, Jouzel J, Raynaud D, et al. (1999) Climate and atmospheric history of the past 420,000 years from the Vostok ice core, Antarctica. *Nature* 399(6735): 429–436. https://doi.org/10.1038/20859.
Piccione G, Blackburn T, Tulaczyk S, et al. (2022) Subglacial precipitates record Antarctic ice sheet response to late pleistocene millennial climate cycles. *Nature Communications* 13(1): 5428. https://doi.org/10.1038/s41467-022-33009-1.
Pilgrim L (1904) Versuch Einer Rechnerischen Behandlung Des Eiszeitproblems. *Jahreshefte Für Vaterländische Naturkunde in Württemberg* 60.
Piotrowski JA and Tulaczyk S (1999) Subglacial conditions under the last ice sheet in Northwest Germany: Ice-bed separation and enhanced basal sliding? *Quaternary Science Reviews* 18(6): 737–751. https://doi.org/10.1016/S0277-3791(98)00042-0.
Pollard D and DeConto RM (2005) Hysteresis in Cenozoic Antarctic ice-sheet variations. *Global and Planetary Change* 45(1–3): 9–21. https://doi.org/10.1016/j.gloplacha.2004.09.011.
Pollard D and DeConto RM (2012) A simple inverse method for the distribution of basal sliding coefficients under ice sheets, applied to Antarctica. *The Cryosphere* 6(5): 953–971. https://doi.org/10.5194/tc-6-953-2012.
Pouillet C (1827) *Éléments de Physique Expérimentale et de Météorologie*. Béchet Jeune.
Pouillet C (1838) Mémoire Sur La Chaleur Solaire, Sur Les Pouvoirs Rayonnants et Absorbants de l'air Atmosphérique et Sur La Température de l'espace. *Comptes Rendus Des Séances Del'Acadeémie de Sciences* 7(24).
Prentice IC, Sykes MT, Lautenschlager M, Harrison SP, Denissenko O, and Bartlein PJ (1993) Modelling global vegetation patterns and terrestrial carbon storage at the last glacial maximum. *Global Ecology and Biogeography Letters* 3(3): 67. https://doi.org/10.2307/2997548.
Rae JWB and Broecker W (2018) What fraction of the pacific and Indian Oceans' deep water is formed in the Southern Ocean? *Biogeosciences* 15(12): 3779–3794. https://doi.org/10.5194/bg-15-3779-2018.
Rae JWB, Burke A, Robinson LF, et al. (2018) CO2 storage and release in the deep Southern Ocean on millennial to centennial timescales. *Nature* 562(7728): 569–573. https://doi.org/10.1038/s41586-018-0614-0.
Rafter PA, Gray WR, Hines SKV, et al. (2022) Global reorganization of deep-sea circulation and carbon storage after the last ice age. *Science Advances* 8(46). https://doi.org/10.1126/sciadv.abq5434. eabq5434.
Rahmstorf S (1995) Bifurcations of the Atlantic thermohaline circulation in response to changes in the hydrological cycle. *Nature* 378(6553): 145–149. https://doi.org/10.1038/378145a0.
Rahmstorf S (1996) On the freshwater forcing and transport of the Atlantic thermohaline circulation. *Climate Dynamics* 12(12): 799–811. https://doi.org/10.1007/s003820050144.
Rainey RCT (2021) *The Earths Long-Term Climate Changes and Ice Ages: A Derivation of Milankovitch Cycles from First Principles*. Version 3. Preprint, arXiv, https://doi.org/10.48550/ARXIV.2011.03985.
Rainey RCT (2022) Long-term changes in the Earth's climate: Milankovitch cycles as an exercise in classical mechanics. *American Journal of Physics* 90(11): 848–856. https://doi.org/10.1119/10.0013563.
Raymo ME (1997) The timing of major climate terminations. *Paleoceanography* 12(4): 577–585. https://doi.org/10.1029/97PA01169.
Raymo ME, Lisiecki LE, and Nisancioglu KH (2006) Plio-Pleistocene ice volume, Antarctic climate, and the global $\delta^{18}o$ record. *Science* 313(5786): 492–495. https://doi.org/10.1126/science.1123296.
Raynaud D and Barnola JM (1985) An Antarctic ice core reveals atmospheric CO_2 variations over the past few centuries. *Nature* 315(6017): 309–311. https://doi.org/10.1038/315309a0.
Raynaud D, Delmas R, Ascencio JM, and Legrand M (1982) Gas extraction from polar ice cores: A critical issue for studying the evolution of atmospheric CO_2 and ice-sheet surface elevation. *Annals of Glaciology* 3: 265–268. https://doi.org/10.3189/S0260305500002895.
Rechid D, Raddatz TJ, and Jacob D (2009) Parameterization of snow-free land surface albedo as a function of vegetation phenology based on MODIS data and applied in climate modelling. *Theoretical and Applied Climatology* 95(3–4): 245–255. https://doi.org/10.1007/s00704-008-0003-y.
Reyes AV, Carlson AE, Clark J, et al. (2024) Timing of Cordilleran-Laurentide ice-sheet separation: Implications for sea-level rise. *Quaternary Science Reviews* 328: 108554. https://doi.org/10.1016/j.quascirev.2024.108554.
Rial JA, Jeseung O, and Reischmann E (2013) Synchronization of the climate system to eccentricity forcing and the 100,000-year problem. *Nature Geoscience* 6(4): 289–293. https://doi.org/10.1038/ngeo1756.
Ridgwell AJ, Watson AJ, and Raymo ME (1999) Is the spectral signature of the 100 Kyr glacial cycle consistent with a Milankovitch origin? *Paleoceanography* 14(4): 437–440. https://doi.org/10.1029/1999PA900018.

Riechers K, Mitsui T, Boers N, and Ghil M (2022) Orbital insolation variations, intrinsic climate variability, and quaternary glaciations. *Climate of the Past* 18(4): 863–893. https://doi.org/10.5194/cp-18-863-2022.

Robinson LF, Adkins JF, Keigwin LD, et al. (2005) Radiocarbon variability in the western North Atlantic during the last deglaciation. *Science* 310(5753): 1469–1473. https://doi.org/10.1126/science.1114832.

Rohling EJ, Marino G, Foster GL, Goodwin PA, Von Der Heydt AS, and Köhler P (2018) Comparing climate sensitivity, past and present. *Annual Review of Marine Science* 10(1): 261–288. https://doi.org/10.1146/annurev-marine-121916-063242.

Ruddiman WF, Raymo M, and McIntyre A (1986) Matuyama 41,000-year cycles: North Atlantic Ocean and Northern Hemisphere Ice Sheets. *Earth and Planetary Science Letters* 80(1–2): 117–129. https://doi.org/10.1016/0012-821X(86)90024-5.

Saltzman B and Maasch KA (1988) Carbon cycle instability as a cause of the late Pleistocene ice age oscillations: Modeling the asymmetric response. *Global Biogeochemical Cycles* 2(2): 177–185. https://doi.org/10.1029/GB002i002p00177.

Sarmiento JL and Toggweiler JR (1984) A new model for the role of the oceans in determining atmospheric P CO_2. *Nature* 308(5960): 621–624. https://doi.org/10.1038/308621a0.

Schimper KF (1837) *Auszug Aus Dem Briefe Des H. Dr Schimper: Über Die Eiszeit*. Allgemeine Schweizerische Gesellschaft für die Gesammten. *Naturwissenschaften*. https://doi.org/10.5169/SEALS-89706.

Schoof C (2007) Ice sheet grounding line dynamics: Steady states, stability, and hysteresis. *Journal of Geophysical Research: Earth Surface* 112(F3). https://doi.org/10.1029/2006JF000664. 2006JF000664.

Seidov D and Maslin M (2001) Atlantic ocean heat piracy and the bipolar climate see-saw during Heinrich and Dansgaard–Oeschger events. *Journal of Quaternary Science* 16(4): 321–328. https://doi.org/10.1002/jqs.595.

Sellers WD (1969) A global climatic model based on the energy balance of the Earth-atmosphere system. *Journal of Applied Meteorology* 8(3): 392–400. https://doi.org/10.1175/1520-0450(1969)008%253C0392:AGCMBO%253E2.0.CO;2.

Shackleton NJ (1977) Carbon-13 in Uvigerina: Tropical rainforest history and the equatorial pacific carbonate dissolution cycles. In: *The Fate of Fossil Fuel C02 in the Oceans*. Plenum.

Shackleton NJ (2000) The 100,000-year ice-age cycle identified and found to lag temperature, carbon dioxide, and orbital eccentricity. *Science* 289(5486): 1897–1902. https://doi.org/10.1126/science.289.5486.1897.

Shakun JD, Clark PU, He F, et al. (2012) Global warming preceded by increasing carbon dioxide concentrations during the last deglaciation. *Nature* 484(7392): 49–54. https://doi.org/10.1038/nature10915.

Sherwood SC, Webb MJ, Annan JD, et al. (2020) An assessment of Earth's climate sensitivity using multiple lines of evidence. *Reviews of Geophysics* 58(4). https://doi.org/10.1029/2019RG000678.

Siegenthaler U and Wenk T (1984) Rapid atmospheric CO2 variations and ocean circulation. *Nature* 308(5960): 624–626. https://doi.org/10.1038/308624a0.

Siegenthaler U, Stocker TF, Monnin E, et al. (2005) Stable carbon cycle–climate relationship during the late Pleistocene. *Science* 310: 6.

Sigman DM and Boyle EA (2000) Glacial/interglacial variations in atmospheric carbon dioxide. *Nature* 407(6806): 859–869. https://doi.org/10.1038/35038000.

Sigman DM and Hain MP (2024) Ocean oxygen, preformed nutrients, and the cause of the lower carbon dioxide concentration in the atmosphere of the last glacial maximum. *Paleoceanography and Paleoclimatology* 39(1). https://doi.org/10.1029/2023PA004775. e2023PA004775.

Sigman DM, McCorkle DC, and Martin WR (1998) The calcite lysocline as a constraint on glacial/interglacial low-latitude production changes. *Global Biogeochemical Cycles* 12(3): 409–427. https://doi.org/10.1029/98GB01184.

Sigman DM, Lehman SJ, and Oppo DW (2003) Evaluating mechanisms of nutrient depletion and ^{13}C enrichment in the intermediate-depth Atlantic during the last ice age. *Paleoceanography* 18, no. 3. https://doi.org/10.1029/2002PA000818. 2002PA000818.

Sigman DM, De Boer AM, and Haug GH (2007) Antarctic stratification, atmospheric water vapor, and Heinrich events: A hypothesis for late Pleistocene deglaciations. In: Schmittner A, Chiang JCH, and Hemming SR (eds.) *Geophysical Monograph Series*, vol. 173. American Geophysical Union. https://doi.org/10.1029/173GM21.

Sigman DM, Hain MP, and Haug GH (2010) The polar ocean and glacial cycles in atmospheric CO2 concentration. *Nature* 466(7302): 47–55. https://doi.org/10.1038/nature09149.

Sigman DM, Fripiat F, Studer AS, et al. (2021) The Southern Ocean during the ice ages: A review of the Antarctic surface isolation hypothesis, with comparison to the north pacific. *Quaternary Science Reviews* 254: 106732. https://doi.org/10.1016/j.quascirev.2020.106732.

Snoll B, Ivanovic R, Gregoire L, et al. (2024) A multi-model assessment of the early last deglaciation (PMIP4 LDv1): A meltwater perspective. *Climate of the Past* 20(4): 789–815. https://doi.org/10.5194/cp-20-789-2024.

Sowers T and Bender M (1995) Climate records covering the last deglaciation. *Science* 269(5221): 210–214. https://doi.org/10.1126/science.269.5221.210.

Stauffer B, Hofer H, Oeschger H, Schwander J, and Siegenthaler U (1984) Atmospheric CO_2 concentration during the last glaciation. *Annals of Glaciology* 5: 160–164. https://doi.org/10.3189/1984AoG5-1-160-164.

Stephens BB and Keeling RF (2000) The influence of Antarctic sea ice on glacial–interglacial CO2 variations. *Nature* 404(6774): 171–174. https://doi.org/10.1038/35004556.

Stocker TF and Johnsen SJ (2003) A minimum thermodynamic model for the bipolar seesaw. *Paleoceanography* 18(4). https://doi.org/10.1029/2003PA000920. 2003PA000920.

Stockwell JN (1873) *Memoir on the Secular Variations of the Elements of the Orbits of the Eight Principal Planets: Mercury, Venus, the Earth, Mars, Jupiter, Saturn, Uranus, and Neptune*, vol. 18. Smithsonian Institution.

Stommel H (1948) The westward intensification of wind-driven ocean currents. *Eos, Transactions American Geophysical Union* 29(2): 202–206. https://doi.org/10.1029/TR029i002p00202.

Stommel H and Arons AB (1959) On the abyssal circulation of the world ocean — II. An idealized model of the circulation pattern and amplitude in oceanic basins. *Deep Sea Research (1953)* 6: 217–233. https://doi.org/10.1016/0146-6313(59)90075-9.

Storch H v and Zwiers FW (1999) *Statistical Analysis in Climate Research*. Cambridge University Press, ISBN: 978-0-521-45071-3.

Studer AS, Sigman DM, Martínez-García A, et al. (2015) Antarctic zone nutrient conditions during the last two glacial cycles. *Paleoceanography* 30(7): 845–862. https://doi.org/10.1002/2014PA002745.

Suwa M and Bender ML (2008) Chronology of the Vostok ice core constrained by O_2/N_2 ratios of occluded air, and its implication for the Vostok climate records. *Quaternary Science Reviews* 27(11–12): 1093–1106. https://doi.org/10.1016/j.quascirev.2008.02.017.

Sverdrup HU (1947) Wind-driven currents in a baroclinic ocean; with application to the equatorial currents of the eastern pacific. *Proceedings of the National Academy of Sciences* 33(11): 318–326. https://doi.org/10.1073/pnas.33.11.318.

Talley LD (2011) *Descriptive Physical Oceanography*. Elsevier. https://doi.org/10.1016/C2009-0-24322-4.

Talley L (2013) Closure of the global overturning circulation through the Indian, Pacific, and Southern oceans: Schematics and transports. *Oceanography* 26(1): 80–97. https://doi.org/10.5670/oceanog.2013.07.

Thompson R (2021) Croll, feedback mechanisms, climate change and the future. *Earth and Environmental Science Transactions of the Royal Society of Edinburgh* 112(3–4): 287–304. https://doi.org/10.1017/S1755691021000153.

Thornalley DJR, Barker S, Broecker WS, Elderfield H, and Nick McCave I (2011) The deglacial evolution of north Atlantic deep convection. *Science* 331(6014): 202–205. https://doi.org/10.1126/science.1196812.

Tierney JE, Zhu J, King J, Malevich SB, Hakim GJ, and Poulsen CJ (2020) Glacial cooling and climate sensitivity revisited. *Nature* 584(7822): 569–573. https://doi.org/10.1038/s41586-020-2617-x.

Timmermann A, Lorenz SJ, An S-I, Clement A, and Xie S-P (2007) The effect of orbital forcing on the mean climate and variability of the tropical pacific. *Journal of Climate* 20(16): 4147–4159. https://doi.org/10.1175/JCLI4240.1.

Toggweiler JR (1999) Variation of atmospheric CO_2 by ventilation of the ocean's deepest water. *Paleoceanography* 14(5): 571–588. https://doi.org/10.1029/1999PA900033.

Toggweiler JR (2008) Origin of the 100,000-year timescale in Antarctic temperatures and atmospheric CO_2. *Paleoceanography* 23(2). https://doi.org/10.1029/2006PA001405. 2006PA001405.

Toggweiler JR and Samuels B (1995) Effect of drake passage on the global thermohaline circulation. *Deep Sea Research Part I: Oceanographic Research Papers* 42(4): 477–500. https://doi.org/10.1016/0967-0637(95)00012-U.

Toggweiler JR and Sarmiento JL (1985) Glacial to interglacial changes in atmospheric carbon dioxide: The critical role of ocean surface water in high latitudes. In: Sundquist ET and Broecker WS (eds.) *Geophysical Monograph Series*. American Geophysical Union. https://doi.org/10.1029/GM032p0163.

Toggweiler JR, Russell JL, and Carson SR (2006) Midlatitude westerlies, atmospheric CO_2, and climate change during the ice ages: Westerlies And CO_2 during the ice ages. *Paleoceanography* 21(2). https://doi.org/10.1029/2005PA001154.

Torell O (1872) Undersökningar Över Istiden 1. *Öfversikt Af Kongliga Vetenskapsakademiens Handlingar*: 25–66.

Torell O (1873) Undersökningar Över Istiden 2. *Öfversikt Af Kongliga Vetenskapsakademiens Handlingar*: 47–64.

Torell O (1875) Protokoll Der November Sitzung 1875. *Zeitschrift Der Deutschen Geologische Gesellschaft (Berlin)* 27: 961–962.

Trenberth KE (2022) *The Changing Flow of Energy Through the Climate System*, 1st edn. Cambridge University Press. https://doi.org/10.1017/9781108979030.

Tyndall J (1860) Note on the transmission of radiant heat through gaseous bodies. *Proceedings of the Royal Society of London (London)* 10: 37–39. https://doi.org/10.1098/rspl.1859.0017.

Tzedakis PC, Crucifix M, Mitsui T, and Wolff EW (2017) A simple rule to determine which insolation cycles lead to interglacials. *Nature* 542(7642): 427–432. https://doi.org/10.1038/nature21364.

Tziperman E, Raymo ME, Huybers P, and Wunsch C (2006) Consequences of pacing the pleistocene 100 Kyr ice ages by nonlinear phase locking to Milankovitch forcing. *Paleoceanography* 21(4). https://doi.org/10.1029/2005PA001241. 2005PA001241.

Ullman DJ, LeGrande AN, Carlson AE, Anslow FS, and Licciardi JM (2014) Assessing the impact of Laurentide ice sheet topography on glacial climate. *Climate of the Past* 10(2): 487–507. https://doi.org/10.5194/cp-10-487-2014.

Van Breedam J, Huybrechts P, and Crucifix M (2023) Hysteresis and orbital pacing of the early cenozoic Antarctic ice sheet. *Climate of the Past* 19(12): 2551–2568. https://doi.org/10.5194/cp-19-2551-2023.

Venetz I (1833) Mémoire Sur Les Variations de La Température Dans Les Alpes de La Suisse. *Denkschriften Der Allgemeinen Schweizerischen Gesellschaft Für Die Gesammten. Naturwissenschaften* 1(2).

Vollmer TD, Ito T, and Lynch-Stieglitz J (2022) Proxy-based preformed phosphate estimates point to increased biological pump efficiency as primary cause of last glacial maximum CO_2 drawdown. *Paleoceanography and Paleoclimatology* 37(11). https://doi.org/10.1029/2021PA004339. e2021PA004339.

Wang YJ, Cheng H, Edwards RL, et al. (2001) A high-resolution absolute-dated late pleistocene monsoon record from Hulu cave, China. *Science* 294(5550): 2345–2348. https://doi.org/10.1126/science.1064618.

Wang Y, Hai Cheng R, Edwards L, et al. (2005) The Holocene Asian monsoon: Links to solar changes and North Atlantic climate. *Science* 308(5723): 854–857. https://doi.org/10.1126/science.1106296.

Wang Y, Cheng H, Lawrence Edwards R, et al. (2008) Millennial- and orbital-scale changes in the East Asian monsoon over the past 224,000 years. *Nature* 451(7182): 1090–1093. https://doi.org/10.1038/nature06692.

Wang XT, Sigman DM, Prokopenko MG, et al. (2017) Deep-sea coral evidence for lower southern ocean surface nitrate concentrations during the last ice age. *Proceedings of the National Academy of Sciences* 114(13): 3352–3357. https://doi.org/10.1073/pnas.1615718114.

Watson AJ, Naveira AC, and Garabato. (2006) The role of southern ocean mixing and upwelling in glacial-interglacial atmospheric CO_2 change. *Tellus B: Chemical and Physical Meteorology* 58(1): 73. https://doi.org/10.1111/j.1600-0889.2005.00167.x.

Wegener A (1929) Die Entstehung Der Kontinente Und Ozeane. In: Westphal W (ed.) *Die Wissenshaft*, 4th edn, vol. 66. Vieweg & Sohn AG. https://doi.org/10.2307/1781265.

Wiener N (1923) Differential-space. *Journal of Mathematics and Physics* 2(1–4): 131–174. https://doi.org/10.1002/sapm192321131.

Willeit M, Ganopolski A, Calov R, and Brovkin V (2019) Mid-Pleistocene transition in glacial cycles explained by declining CO_2 and regolith removal. *Science Advances* 5(4). https://doi.org/10.1126/sciadv.aav7337. eaav7337.

Winterfeld M, Mollenhauer G, Dummann W, et al. (2018) Deglacial mobilization of pre-aged terrestrial carbon from degrading permafrost. *Nature Communications* 9(1): 3666. https://doi.org/10.1038/s41467-018-06080-w.

Wu Y, Malinverno A, Meyers SR, and Hinnov LA (2024) A 650-Myr history of Earth's axial precession frequency and the evolution of the Earth-Moon system derived from cyclostratigraphy. *Science Advances* 10(42). https://doi.org/10.1126/sciadv.ado2412. eado2412.

Yun K-S, Timmermann A, Lee S-S, Willeit M, Ganopolski A, and Jadhav J (2023) A transient coupled general circulation model (CGCM) simulation of the past 3 million years. *Climate of the Past* 19(10): 1951–1974. https://doi.org/10.5194/cp-19-1951-2023.

Zhang Z, Huang Y, Ma C, et al. (2025) 100-Kyr climate cycles caused by 2.4-Myr eccentricity-modulated carbon cycles. *Nature Communications* 16(1): 8043. https://doi.org/10.1038/s41467-025-63403-4.

Zhu J and Poulsen CJ (2021) Last glacial maximum (LGM) climate forcing and ocean dynamical feedback and their implications for estimating climate sensitivity. *Climate of the Past* 17(1): 253–267. https://doi.org/10.5194/cp-17-253-2021.

CLSS: 00056

Non-Print Items

Keywords: Atlantic meridional overturning circulation AMOC; Carbon dioxide CO_2; Chaos; Climate feedback; Climate forcing; Climate memory; Climate system; Climate variability; Deep ocean ventilation; Ddeglacial; Deterministic; Dynamics; Earth System Science; Eccentricity; Glacial; Greenhouse effect; Greenhouse gas; History of science; Ice ages; Ice sheets; Insolation; Interglacial; Millennial timescale; Milutin Milankovitch; Obliquity; Ocean circulation; Orbital cycles; Precession; Southern Ocean; Stochastic forcing; Weather